

PB 284 201

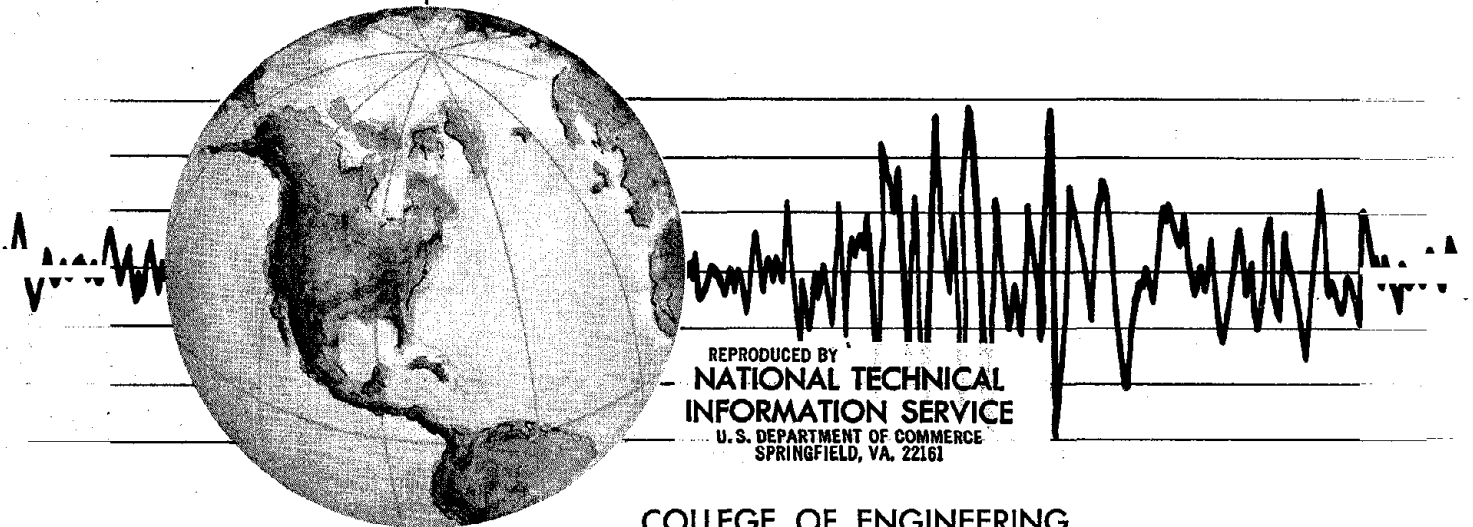
REPORT NO.
UCB/EERC-77/14
JUNE 1977

EARTHQUAKE ENGINEERING RESEARCH CENTER

SEISMIC STRAIN INDUCED IN THE GROUND DURING EARTHQUAKES

by
YOSHIHIRO SUGIMURA

Report to National Science Foundation



REPRODUCED BY
NATIONAL TECHNICAL
INFORMATION SERVICE
U. S. DEPARTMENT OF COMMERCE
SPRINGFIELD, VA. 22161

COLLEGE OF ENGINEERING
UNIVERSITY OF CALIFORNIA • Berkeley, California

4 4

Vertical line of text or scanning artifacts on the right edge of the page.

Horizontal line at the bottom left corner.

SEISMIC STRAIN
INDUCED IN THE GROUND
DURING EARTHQUAKES

by

Yoshihiro Sugimura

Report No. UCB/EERC-77/14
Earthquake Engineering Research Center
College of Engineering
University of California
Berkeley, California

June 1977



BIBLIOGRAPHIC DATA SHEET	1. Report No. NSF/RA-770558	2.	3. Recipient's Accession No. PR284201	
4. Title and Subtitle Seismic Strain Induced in the Ground During Earthquakes			5. Report Date June 1977	6.
7. Author(s) Yoshihiro Sugimura			8. Performing Organization Rept. No. UCB/EERC-77/14	
9. Performing Organization Name and Address Earthquake Engineering Research Center University of California, Richmond Field Station 47th and Hoffman Blvd. Richmond, California 94804			10. Project/Task/Work Unit No.	
12. Sponsoring Organization Name and Address National Science Foundation 1800 G Street, N.W. Washington, D. C. 20550			11. Contract/Grant No. ENV 76-04264 A02	
15. Supplementary Notes			13. Type of Report & Period Covered	
16. Abstracts			14.	
<p>This report develops a method of estimating seismic ground strain by using techniques for strong motion data and presents some computed results from these techniques. Simple plane wave forms are applied to seismic records for an estimation of strain.</p> <p>The two earthquakes selected for this study have shallow focal depths and strong ground motions. For these earthquakes the parallel and normal directions to the causative fault line are shown to form a pair of orthogonal axes, along which the mean square intensities of the components of ground motion have maximum and minimum values.</p> <p>The velocity curves are transformed to this coordinate system. Then the seismic shear strain component at each frequency is evaluated by applying Fourier analysis and the simple plane wave solution.</p>				
17b. Identifiers/Open-Ended Terms				
17c. COSATI Field/Group				
18. Availability Statement Release Unlimited			19. Security Class (This Report) UNCLASSIFIED	21.
ia			20. Security Class (This Page) UNCLASSIFIED	22. Price PC A04/A01

du-
ele
t

ABSTRACT

This report develops a method of estimating seismic ground strain by using techniques for strong motion data and presents some computed results from these techniques. Simple plane wave forms are applied to seismic records for an estimation of strain.

The two earthquakes selected for this study have shallow focal depths and strong ground motions. For these earthquakes the parallel and normal directions to the causative fault line are shown to form a pair of orthogonal axes, along which the mean square intensities of the components of ground motion have maximum and minimum values.

The velocity curves are transformed to this coordinate system. Then the seismic shear strain component at each frequency is evaluated by applying Fourier analysis and the simple plane wave solution.

TABLE OF CONTENTS

	<u>page</u>
TABLE OF CONTENTS	iii
ACKNOWLEDGEMENTS	v
LIST OF FIGURES	vii
LIST OF TABLES	xi
INTRODUCTION	1
DETERMINATION OF STRAIN	1
EARTHQUAKE WAVES USED AS EXAMPLES.	4
LONGITUDINAL AND TRANSVERSE COMPONENTS	5
FOURIER ANALYSIS	8
NORMAL AND PARALLEL COMPONENTS TO THE FAULT LINE	10
ESTIMATION OF SEISMIC SHEAR STRAIN	12
CONCLUSIONS.	13
REFERENCES	45
APPENDIX	49

Preceding page blank

ACKNOWLEDGEMENTS

This research was done with the kind support and assistance of Professor J. Penzien, University of California, Berkeley; the author wishes to acknowledge his considerable help.

The author would also like to express his thanks to Professor Y. Ohsaki, University of Tokyo, for the use of some subroutine sub-programs coded by him.

The author also wishes to thank Dr. Beverley Bolt for reviewing the manuscript, Mrs. Abby Burton for typing the manuscript and Ms. Gail Fezell for drafting the figures.

The financial support provided by the National Science Foundation under grant No. ENV 76-04264 A02 is gratefully acknowledged.

LIST OF FIGURES

		<u>page</u>
Fig. 1	Schematic location map of station, epicenter and causative fault (Imperial Valley Earthquake).	15
Fig. 2	Schematic location map of station, epicenter and causative fault (Kern County Earthquake)	16
Fig. 3	Transformation of coordinates	17
Fig. 4	Relation between components of seismograph and transformed coordinates (Imperial Valley Earthquake) . . .	18
Fig. 5	Relation between components of seismograph and transformed coordinates (Kern County Earthquake).	18
Fig. 6	Reproduced acceleration curves in longitudinal and transverse directions (Imperial Valley Earthquake) . .	19
Fig. 7	Reproduced velocity curves in longitudinal and transverse directions (Imperial Valley Earthquake)	19
Fig. 8	Reproduced acceleration curves in longitudinal and transverse directions (Kern County Earthquake)	20
Fig. 9	Reproduced velocity curves in longitudinal and transverse directions (Kern County Earthquake)	20
Fig. 10	Particle velocity orbit for first 6 seconds at Imperial Valley Irrigation District	21
Fig. 11	Particle velocity orbit for first 4.8 seconds at Taft Lincoln School Tunnel	22
Fig. 12	Fourier amplitudes of longitudinal and transverse components relative to the direction from the epicenter - El Centro 0 - 50 sec.	23
Fig. 13a	Fourier amplitudes of longitudinal and transverse components relative to the direction from the epicenter - El Centro 0 - 10 sec.	23
Fig. 13b	Fourier amplitudes of longitudinal and transverse components relative to the direction from the epicenter - El Centro 10 - 30 sec.	24
Fig. 13c	Fourier amplitudes of longitudinal and transverse components relative to the direction from the epicenter - El Centro 30 - 50 sec.	24
Fig. 14	Fourier amplitudes of transverse and corrected longitudinal components relative to the direction from the epicenter - Taft 0 - 50 sec.	25

Fig. 15a	Fourier amplitudes of transverse and corrected longitudinal components relative to the direction from the epicenter - Taft 0 - 10 sec.	25
Fig. 15b	Fourier amplitudes of transverse and corrected longitudinal components relative to the direction from the epicenter - Taft 10 - 30 sec.	26
Fig. 15c	Fourier amplitudes of transverse and corrected longitudinal components relative to the direction from the epicenter - Taft 30 - 50 sec.	26
Fig. 16	Reproduced acceleration curves in normal and parallel directions (Imperial Valley Earthquake)	27
Fig. 17	Reproduced velocity curves in normal and parallel directions (Imperial Valley Earthquake)	27
Fig. 18	Reproduced acceleration curves in normal and parallel directions (Kern County Earthquake)	28
Fig. 19	Reproduced velocity curves in normal and parallel directions (Kern County Earthquake)	28
Fig. 20	Schematic explanation of coordinate transformation	29
Fig. 21	Fourier amplitudes of parallel and corrected normal components in the direction of the fault line - El Centro 0 - 50 sec.	30
Fig. 22a	Fourier amplitudes of parallel and corrected normal components in the direction of the fault line - El Centro 0 - 10 sec.	30
Fig. 22b	Fourier amplitudes of parallel and corrected normal components in the direction of the fault line - El Centro 10 - 30 sec.	31
Fig. 22c	Fourier amplitudes of parallel and corrected normal components in the direction of the fault line - El Centro 30 - 50 sec.	31
Fig. 23	Fourier amplitudes of parallel and corrected normal components in the direction of the fault line - Taft 0 - 50 sec.	32
Fig. 24a	Fourier amplitudes of parallel and corrected normal components in the direction of the fault line - Taft 0 - 10 sec.	32
Fig. 24b	Fourier amplitudes of parallel and corrected normal components in the direction of the fault line - Taft 10 - 30 sec.	33

Fig. 24c Fourier amplitudes of parallel and corrected
normal components in the direction of the fault
line - Taft 30 - 50 sec. 33



LIST OF TABLES

		<u>page</u>
Table 1	Properties of Earthquakes and Stations	35
Table 2	Subsurface Unit Thickness and Seismic Data at Each Station (After Duke and Leeds, 1962)	36
Table 3	Maximum Value and Occurrence Time, Longitudinal and Transverse Components	37
Table 4	Conditions of Computation and Corresponding Figure Number	38
Table 5	Peak Fourier Amplitude and Frequency of Transverse Component at El Centro Site	39
Table 6	Peak Fourier Amplitude and Frequency of Transverse Component at Taft Site	39
Table 7	Maximum Value and Occurrence Time, Normal and Parallel Components	40
Table 8	Peak Fourier Amplitude and Frequency of Parallel Component at El Centro Site	41
Table 9	Peak Fourier Amplitude and Frequency of Parallel Component at Taft Site	41
Table 10	Simplified Seismic Data at El Centro Site	42
Table 11	Simplified Seismic Data at Taft Site	42
Table 12	Estimated Lower and Upper Limit of Shear Strain at El Centro Site	43
Table 13	Estimated Lower and Upper Limit of Shear Strain at Taft Site	43

INTRODUCTION

It is well-known that local soil conditions at sites subjected to seismic shaking considerably affect damage to structures at the site. Many analytical studies and laboratory tests have been performed to determine the dynamic characteristics of various types of soil deposits. In particular "strain dependence" of soils, i.e., nonlinearity of shear modulus and damping ratio with shear strain, has been clarified mainly by laboratory tests [1, 2, 3, 4, 5, 6].* A clue to the relationship between earthquake ground shaking and damage to structures may be found if strains induced in the ground during an earthquake are evaluated and then compared with results from laboratory tests.

An interesting question that also arises is as follows: "How large will the actual strain level in soil layers induced by seismic ground motion be, particularly in the case of a great destructive earthquake?" Strain data obtained directly from instruments in soil deposits would provide the answer. However, except for some geophysical and geotechnical surveys such as triangulation which are mostly in a static sense, no suitable instruments equivalent to strong-motion accelerographs for ground acceleration have been developed to measure local seismic strain waves.

This report develops a method of estimating seismic ground strain by using techniques for strong motion data and presents some computed results from these techniques. Although the depth of soils, especially soft soils, is a significant factor [7, 8] it is beyond the scope of this paper.

DETERMINATION OF STRAIN

First, consider a plane wave in an elastic homogeneous body. If the wave is a shear wave, particle motion in the body is transverse to the direction of propagation and if it is a compressional wave, particle motion

*Numbers in square brackets refer to corresponding references.

is parallel to the direction of propagation (longitudinal). If the x and y axes are chosen in the longitudinal and transverse directions, respectively, and u and v are the corresponding particle displacements, then the fundamental wave propagation equations can be represented as follows:

For a longitudinal wave,

$$\frac{\partial^2 u}{\partial t^2} = c_1^2 \frac{\partial^2 u}{\partial x^2} \quad (1)$$

and for a transverse wave,

$$\frac{\partial^2 v}{\partial t^2} = c_2^2 \frac{\partial^2 v}{\partial x^2} \quad ; \quad (2)$$

where

$$c_1 = V_p = \left[\frac{E}{\rho} \frac{1-\nu}{(1+\nu)(1-2\nu)} \right]^{\frac{1}{2}} \quad (3)$$

and

$$c_2 = V_s = \left[\frac{G}{\rho} \right]^{\frac{1}{2}} \quad (4)$$

are the longitudinal (or compressional) wave velocity and transverse (or shear) wave velocity, respectively. E, G, and ν are Young's modulus, the shear modulus and Poisson's ratio of the elastic body, respectively. Equations (1) and (2) have similar solutions of the form

$$D = f(x-ct) + g(x+ct) \quad (5)$$

where D and c are either u and c_1 or v and c_2 , respectively. The first term on the right hand side of eq. (5) represents a forward moving wave and the second term a backward moving wave. If the elastic body is infinite or if the effects of reflected waves from a boundary can be neglected, then it is only necessary to consider the forward wave to determine the behavior of an arbitrary point in the body, so that

$$D = f(x-ct) \quad (6)$$

The particle velocity and strain at that location are obtained by differentiating eq. (6) with respect to t and x as shown below,

$$\dot{D} = \frac{dD}{dt} = -cf'(x-ct) \quad (7)$$

$$\varepsilon = \frac{dD}{dx} = f'(x-ct) \quad (8)$$

Hence

$$\varepsilon = -\frac{\dot{D}}{c} \quad (9)$$

Thus the strain can be simply expressed as the ratio of particle velocity to wave velocity. Therefore, axial and shear strains are shown, respectively, as follows:

$$\varepsilon_x = -\frac{\dot{u}}{c_1} \quad (10)$$

$$\gamma_{xy} = -\frac{\dot{v}}{c_2} \quad (11)$$

It is obvious, furthermore, that the maximum shear velocity \dot{v} of a particle and the maximum shear strain γ_{xy} occur simultaneously when the solution v is expressed by the sinusoidal wave form.

In the case of seismic waves propagating through the earth, conditions are considerably different from the case of plane waves. The following difficulties must be considered.

(1) The energy source may move along a line or on a plane, i.e., an earthquake fault, so that the source is a function of time as well as space.

(2) A variety of properties might be contained within the waves themselves induced from the source. The structure is so complicated that in most cases it is not possible to represent the wave motion exactly by a physical model, therefore measurements of seismic waves will be considered as random quantities.

(3) There exist many soil layers and topographic boundaries in the actual ground at which reflection and refraction of seismic waves might occur.

(4) Parameters such as Young's modulus and the shear modulus of soils will not be constant during a destructive ground shaking since, in general, soils are not elastic.

If an observation station, however, is located far enough from the source, seismic records at that location can be decomposed into different wave components according to the different wave velocities c_1 , c_2 and so on. Based on this possibility, decomposition technique has been used regularly in seismology to overcome to some extent the difficulties (1) and (2). Difficulties (3) and (4) are principally derived from local site conditions extremely near the surface of the earth so that they might not affect significantly arrival times of waves in earlier parts of seismic records. These effects cannot be neglected, however, if it is necessary to consider the amplitudes of recorded waves. It has been pointed out, for instance, that maximum values of ground response to seismic shaking scatter in a remarkably wide range under the influence of local soil conditions [1, 2]. In particular, because of the interdependence between elastic modulus and amplitude of the particle velocity, strains cannot be determined directly from seismic records.

In spite of all these difficulties and uncertainties, the application of the simple plane wave forms (eqs. (10) and (11)) to seismic records for an estimation of strain appears to be, at present, the best available first approximation for engineering use.

EARTHQUAKE WAVES USED AS EXAMPLES

Since the San Fernando earthquake in 1971 during which many seismic records were obtained in Southern California strong motion data from the Western states, including these records, have been processed at the Earthquake Engineering Research Laboratory, California Institute of Technology [9]. Some data processing techniques such as "baseline" correction and

high-frequency correction [10, 11] were applied to these data and, finally, the results were published as corrected accelerograms and integrated ground velocity and displacement curves [12]. The object of the base line correction was to prevent divergence of the resultant curves, which may occur if the original data are integrated simply and directly. The object of the high-frequency correction was to account for the fall-off of basic transducer response in the accelerographs [10, 11, 13].

These corrected data are suitable for the purpose of this work. Two earthquake records were selected from among them and used as shown in Table 1. Schematic maps of locations of the epicenters and recording stations for these earthquakes are shown in Figs. 1 and 2, respectively. Both earthquakes selected have strong ground motions and shallow focal depths as is generally the case in California and the Western states.

Geotechnical data from the sites of the stations are given by C. M. Duke and D. J. Leeds, 1962 [14]; W. R. Hansen et al., 1973 [15]; and the U.S. Department of the Interior, Geological Survey, 1976 [16]. Subsurface unit thickness and seismic data from Duke and Leeds are shown in Table 2, and will be used as basic in subsequent sections.

LONGITUDINAL AND TRANSVERSE COMPONENTS

Since earthquakes occur at random locations, the direction of each component of a seismogram at a station does not ordinarily coincide with the direction to the focus. Therefore, records are initially decomposed into longitudinal and transverse components. Let us consider u , v and w as vector components in the longitudinal, transverse and vertical directions, respectively, and u' , v' and w' as former components. If a_i ($i = 1, 2, 3$) are direction cosines, then

$$u = a_1 u' + a_2 v' + a_3 w' \quad (12)$$

Similarly,

$$v = b_1 u' + b_2 v' + b_3 w' \quad (13)$$

and

$$w = c_1 u' + c_2 v' + c_3 w' \quad (14)$$

in which b_i ($i = 1, 2, 3$) and c_i ($i = 1, 2, 3$) are direction cosines of v and w to u' , v' and w' , respectively.

If the depth of the focus can be neglected or is assumed not to affect the direction of wave propagation, direction cosines a_3 , b_3 , c_1 and c_2 are zero and $c_3 = 1$. Then, eqs. (12) to (14) reduce to the following simple forms.

$$u = a_1 u' + a_2 v' \quad (15)$$

$$v = b_1 u' + b_2 v' \quad (16)$$

$$w = w' \quad (17)$$

Furthermore, since the coordinate systems are Cartesian, eqs. (15) and (16) can be written as

$$\left. \begin{aligned} u &= u' \cos \theta + v' \sin \theta \\ v &= u' \sin \theta + v' \cos \theta \end{aligned} \right\} \quad (-90^\circ < \theta < 90^\circ) \quad (18)$$

We note that it does not necessarily follow that the positive direction of the longitudinal axis coincides with the direction from the station to the focus. For instance, for the Imperial Valley earthquake, the positive direction on the longitudinal axis coincides with the direction to the focus but vice versa for the Kern County earthquake, as shown in Figs. 4 and 5, respectively.

Acceleration and velocity curves in both cases generated by eq. (18) are shown in Figs. 6 to 9. Table 3 shows the maximum values and occurrence times for these curves compared with those of the original records. For the Taft record, there are only slight changes in the maximum values and wave shape, but no change in the occurrence time of the maximum values

since the direction cosines are nearly equal to zero or unity during the coordinate transformation; that is, the new longitudinal curves correspond to the original E-W component and the new transverse curves to the N-S components. On the other hand, in the case of the El Centro record after the coordinate transformation the new curves are different from those of the original records.

Figure 10 shows the particle orbit for the first six seconds based on both components of the transformed velocity curves at the Imperial Irrigation District station in El Centro. Similarly, the particle velocity orbit described for the first 4.8 seconds at Taft Lincoln School Tunnel station is shown in Fig. 11. Approximate directions along the fault lines observed on the ground surface during these earthquakes are also shown in these figures [17, 18]. The direction is shown by a single solid line at the El Centro site because the Imperial fault is running nearly straight (see Fig. 4). For the White Wolf fault in Kern County, the direction can be estimated as almost straight but slightly curved at the southern end near the epicenter (see Fig. 5). Thus two lines are shown in Fig. 11. The solid line shows the direction judged from the whole and the dashed line shows the direction estimated from the vicinity of the observed fault end. What is evident and interesting from these two figures is that large shaking components are induced along the direction of the fault line rather than along the longitudinal or transverse directions to the focus. Horizontal dislocation was predominant in the activity of both the Imperial fault and the White Wolf fault, thus causing strongest motions along their fault lines [19, 20, 21]. Distinctive characteristics of short or medium distance shocks should be considered for these earthquakes because the epicentral distances from the stations are about 7.3 miles (El Centro) and 25.6 miles (Taft), respectively. This fact suggests that for these earthquakes an important factor affecting the ground motion will be the direction of slip of the fault. Hence, it might be more informative to transform the coordinate system to the directions normal and parallel to the fault line. In any case, in order to confirm this suggestion, further research is necessary as well as improved methods of analyzing large quantities of data.

FOURIER ANALYSIS

Fourier analysis provides a powerful means of investigating the characteristics of a random wave in the frequency domain. Let us consider now the components in the frequency domain in the longitudinal and transverse directions. The Fourier amplitudes and phase angles for N discrete data samples X_m with time interval Δt , where N is even, are shown by

$$\left. \begin{aligned} X_k &= [A_k^2 + B_k^2]^{1/2} \\ \phi_k &= \tan^{-1}\left(-\frac{B_k}{A_k}\right) \end{aligned} \right\}, \quad k = 0, 1, 2, \dots, \frac{N}{2} \quad (19)$$

where

$$\left. \begin{aligned} A_k &= \frac{2}{N} \sum_{m=0}^{N-1} X_m \cos \frac{2\pi km}{N} \\ B_k &= \frac{2}{N} \sum_{m=0}^{N-1} X_m \sin \frac{2\pi km}{N} \end{aligned} \right\} \quad (20)$$

Then, the time history of each component of the Fourier transform wave is expressed by

$$X_k(t) = X_k \cos(2\pi f_k t + \phi_k), \quad k = 0, 1, 2, \dots, \frac{N}{2}, \quad (21)$$

where

$$f_k = \frac{k}{N\Delta t} \quad (22)$$

is the frequency of the k^{th} Fourier transform wave. Recalling the definition of

$$C_k = \frac{A_k - iB_k}{2}, \quad k = 0, 1, 2, \dots, N-1 \quad (23)$$

then

$$A_k + iB_k = A_{N-k} - iB_{N-k}, \quad k = 0, 1, 2, \dots, \frac{N}{2}; \quad (24)$$

so that eq. (21) can be expressed in terms of discrete complex Fourier coefficients given by the equation,

$$C_k = \frac{1}{N} \sum_{m=0}^{N-1} X_m e^{-i(2\pi km/N)}, \quad k = 0, 1, 2, \dots, N-1. \quad (25)$$

The discrete Fourier coefficients A_k and B_k are shown as follows:

$$\left. \begin{aligned} A_k &= 2\text{Re}(C_k) \\ B_k &= -2\text{Im}(C_k) \end{aligned} \right\} k = 0, 1, 2, \dots, \frac{N}{2} \quad (26)$$

(This method is the fast Fourier transformation (FFT) [22].) Coefficients C_k were computed first by using a subroutine program of the FFT coded by Y. Ohsaki (see program list in Appendix), then the Fourier amplitudes and phase angles were obtained by eq. (19). These results are shown in Figs. 12 to 13c for the El Centro site, and in Figs. 14 to 15c for the Taft site.

Two approaches were attempted in this computation process: (1) The time duration during which the Fourier analysis is applied is divided into four different parts; viz., the total fifty seconds from the initial time; zero to ten seconds; ten to thirty seconds; and thirty to fifty seconds. The results from the latter three parts correspond to the so-called running Fourier spectrum. (2) Using the phase angle, a correction was made to the Fourier amplitude of the longitudinal component at each frequency so as to satisfy simultaneously the maximum value of the transverse component. The results of these calculations are tabulated in Table 4.

The purpose of these computations is to consider whether there exists a frequency at which either the longitudinal or transverse component shows a high peak and the other a low trough. If this were found in the figures, it could be used to distinguish the kind or type of wave which is the dominant component in the ground motion. For instance, if the transverse component is more dominant than the longitudinal, such a frequency component might be identified as a shear wave and so forth. This idea can also be applied by a statistical approach corresponding to the concept of "principal

axes of ground motion" presented by T. Kubo and J. Penzien [23], although in a slightly different sense.

Each shaded part in Figs. 12 to 15c shows the range where the transverse component becomes larger than the longitudinal. The selection of several peaks for the transverse component from this range was attempted. The results are summarized in Table 5 and Table 6. What is evident here is that the same or a very close frequency component for each peak in the total fifty seconds is clearly confirmed in each of the three intervals. The classification of the wave type, however, is fairly complicated because a low value of the longitudinal component does not always correspond to the peak of the transverse component.

NORMAL AND PARALLEL COMPONENTS TO THE FAULT LINE

In this section let us consider the normal and parallel waves to the fault line reproduced from the original records. The procedure is the same as that described in the preceding sections with the appropriate angle of transformation; i.e., $\theta = +54^\circ.5$ for the El Centro site and $\theta = -40^\circ.4$ for the Taft site, as shown in Table 7. Note that for the Taft site, the direction of the dashed line in Fig. 11 was assumed to be the direction of fault slip in the area nearest to the station.

Figures 16 and 17 show the acceleration and velocity waves for the Imperial Valley earthquake; those of the Kern County earthquake are shown in Figs. 18 and 19. Consider the parallel components of these waves and compare them schematically with the longitudinal and transverse curves shown before (Figs. 6, 7 for the El Centro site and Figs. 8, 9 for the Taft site) and the original north-south and east-west records. Initially we will call these waves SH (parallel), LO (longitudinal), TR (transverse), NS (original north-south) and EW (original east-west).

In the case of the Imperial Valley, if the sign is reversed the form of the SH wave is similar to that of LO even though the values of the amplitudes are different from each other. This tendency is particularly conspicuous in the velocity curves. Now LO was quite different from

either NS or EW, as mentioned before, hence SH bears no resemblance to either NS or EW.

In the case of the Kern County earthquake, it can be seen from Figs. 8 and 18, or Figs. 9 and 19 that SH is not like LO or TR. In particular, the amplitudes are different. Meanwhile LO resembles EW closely and TR resembles NS, as before. Therefore, it can be said that SH bears no resemblance to either NS or EW.

This result can be justified theoretically as follows: Assuming $u' = v' = 1$ and solving eq. (18) for u with $0^\circ < \theta < 45^\circ$, the result shown in Fig. 20 is obtained. The new component u or the ratio $r = u/u'$ (in which $u' = 1$) can be expressed by the length of the chord for values of θ and changes on the continuous curve described in this figure. The range of r is $r = 1$ at $\theta = 0^\circ$ to $r = 2$ at $\theta = 45^\circ$. Three pairs of components corresponding to the smallest rotation angle were selected from among the three coordinates of SH, LO-TR and NS-EW and each ratio was calculated. The results are summarized below.

El Centro site

Case 1	SH to LO	18°.5	$r = 1.266$
Case 2	SH to NS	35°.5	$r = 1.395$
Case 3	LO to EW	36° .0	$r = 1.397$

Taft site

Case 4	SH to LO	43° .0	$r = 1.413$
Case 5	SH to EW	40° .4	$r = 1.409$
Case 6	LO to EW	2° .6	$r = 1.044$

All the other combinations of components have larger ratios than these cases. It is clear from the above that the pairs of waves are similar to each other in Case 1 and especially in Case 6 because of their small ratios, but look quite different from each other in Cases 2, 3, 4 and 5.

Attention should also be paid to the fact that for $\theta = 45^\circ$ one component becomes zero. This fact suggests that there may exist a set of directions of the predominant and minor ground motion that are principal axes. At the same time, it also suggests that it might not be reasonable to use directly the values measured by a seismograph as the ground motion at the site because only in rare cases do the directions of the seismograph agree with these principal axes.

The computed Fourier amplitudes of the parallel and normal velocity waves are shown in Figs. 21 to 22c for the El Centro site and in Figs. 23 to 24c for the Taft site. The computations are the same as before (Table 4); in particular, comparing Fig. 21 with Fig. 12 or Fig. 23 with Fig. 14, for these curves the shaded part is more clearly defined than before. The selection of peaks of the parallel components from among these figures was performed in the same manner as before. The results are summarized in Table 8 and Table 9 for the El Centro and Taft sites, respectively. The peak of the parallel component corresponds to the low trough of the normal component at almost all the frequencies so that the component waves can be identified as shear waves or, at least, waves of shear type. Hence, a coordinate transformation to the normal and parallel directions to the causative fault line rather than to the longitudinal and transverse directions to the epicenter seems to be more satisfactory for explaining the characteristics of ground motion at a station site.

ESTIMATION OF SEISMIC SHEAR STRAIN

From the preceding section, it seems reasonable to assume as a first approximation that each predominant frequency component in the parallel direction is a shear wave. In this section, an estimate of the seismic shear strain in the ground at each site is attempted by applying eq. (11). First the seismic data shown in Table 2 are simplified as follows: At each site some equivalent single soil layers are considered with an average shear wave velocity shown by,

$$\bar{V}_{si} = \frac{\sum V_{si} H_i}{\sum H_i} \quad (27)$$

in which i is the stratum number from the surface and V_{si} and H_i are the

shear wave velocity and the thickness of each stratum, respectively. Then the natural frequency of each equivalent layer is expressed by

$$\bar{f}_i = \frac{4\Sigma H_i}{V_{si}} \quad (28)$$

The average velocity and frequency calculated for each layer from eqs. (27) and (28), respectively, are summarized in Table 10 and Table 11. Five equivalent single layers exist at the El Centro site and four at the Taft site. Next, taking these frequencies as representative boundary values, peak frequency components shown in Table 8 and Table 9 are classified into several groups. Then, shear strains at each site are calculated by eq. (11) for each case using the value \bar{V}_s of the adjacent lower frequency (lower limit of shear strain) and higher frequency (upper limit of shear strain). The results are summarized in Table 12 and Table 13, respectively. Finally, the average value of shear strain corresponding to each frequency will change within the range between these lower and upper limits. The order of these strain levels is estimated as about 10^{-3} (%) at the El Centro site and about 10^{-4} (%) at the Taft site.

The above approach provides a basis for the assumption that each peak seen in Fig. 21 or Fig. 23 corresponds to a single soil layer of some depth for which the first vibration mode corresponds to the particular peak frequency. As is generally known, the first mode of a soil layer is to some extent predominant in the ground motion at a site. Therefore, as a first approximation this assumption will be an effective method of investigating the ground motion. It should be kept in mind, however, that such a method (1) gives the average value through the whole soil deposit; (2) shows only the discrete Fourier amplitude corresponding to each frequency; and (3) gives no consideration to the higher modes of the ground. Hence, further studies such as improvement of the method and analysis of more data are necessary to clarify the real shear strain wave induced in the local part of the ground during earthquakes.

CONCLUSIONS

The conclusions achieved in this work can be divided into the following

two categories.

(1) The mean square intensity of a single orthogonal component of ground motion at a site depends on the direction of that component. There exists a pair of orthogonal axes (principal axes) along which the mean square intensities of the components of motion have maximum and minimum values. The parallel and normal directions to the causative fault line were shown to correspond to such a coordinate system for the two examples of earthquake and station, i.e., Imperial Valley earthquake (1940) recorded at El Centro site and Kern County earthquake (1952) recorded at Taft site. This is consistent with the characteristics of these causative faults, namely that they (a) slip mainly horizontally, and (b) are regarded as nearly straight lines. A more difficult situation will arise in the case of earthquakes caused by faults with more complicated characteristics.

(2) Provided that the velocity curves are transformed to the coordinate system mentioned above and that the predominant components in the parallel direction are assumed to be of shear wave type, it is possible to evaluate the seismic shear strain component at each frequency by applying Fourier analysis and the simple plane wave solution. The order of the average shear strain component at each frequency caused by ground shaking can be estimated at about 10^{-3} (%) at the El Centro site and about 10^{-4} (%) at the Taft site as a first approximation. It should be noted, however, that additional detailed study is necessary to determine the shear strain induced in the ground during an earthquake.

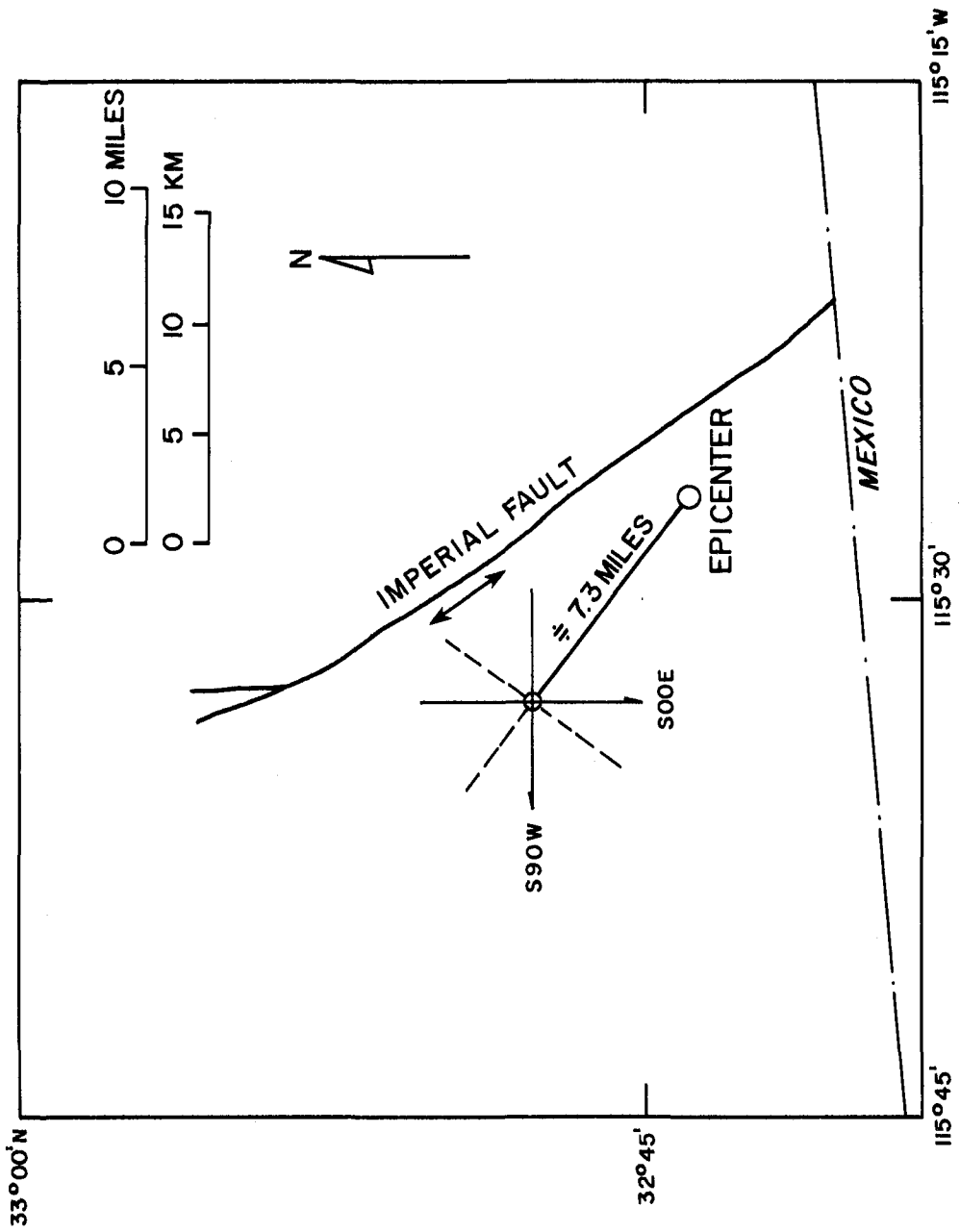


Fig. 1 Schematic location map of station, epicenter and causative fault (Imperial Valley Earthquake)

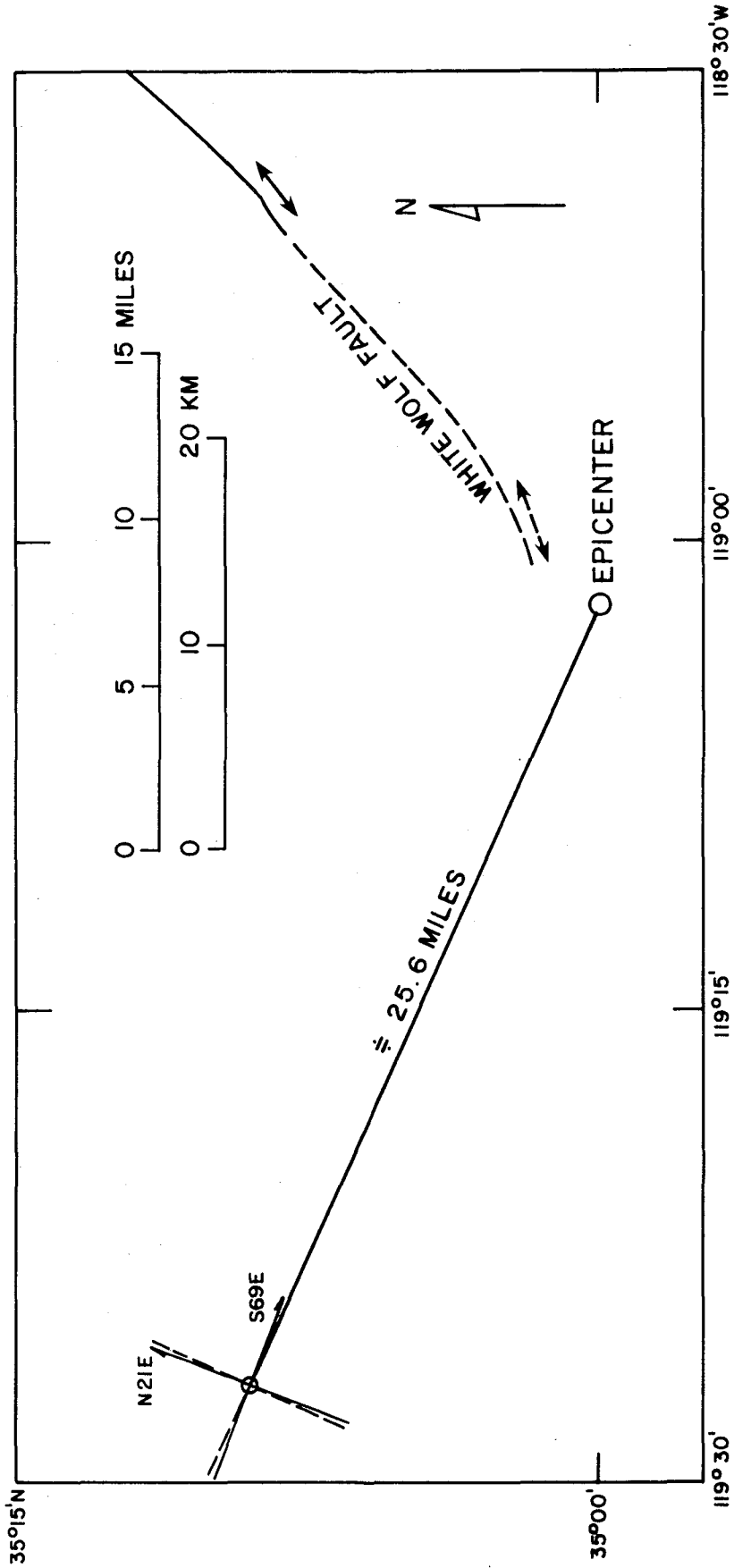


Fig. 2 Schematic location map of station, epicenter and causative fault (Kern County Earthquake)

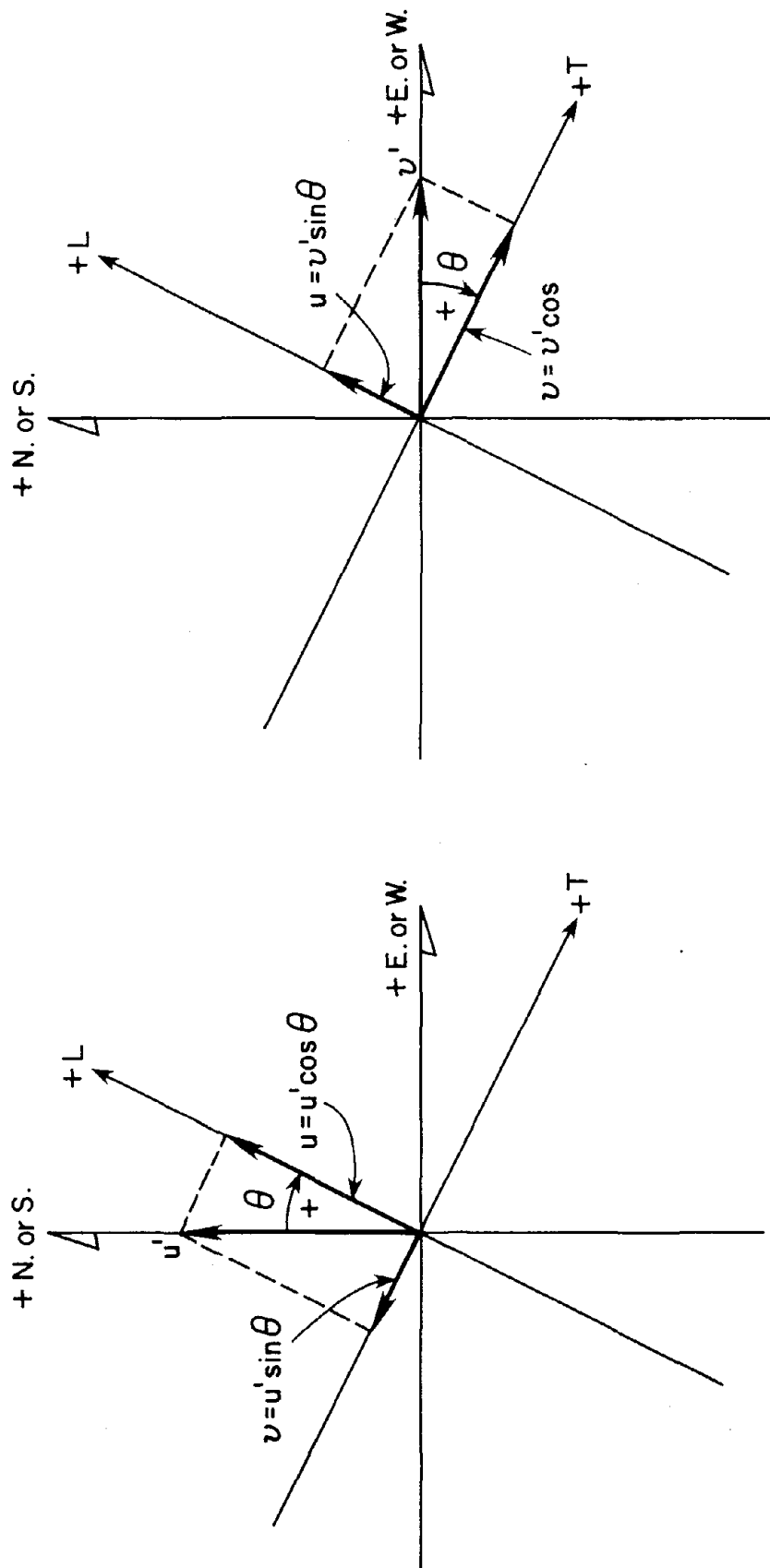


Fig. 3 Transformation of coordinates

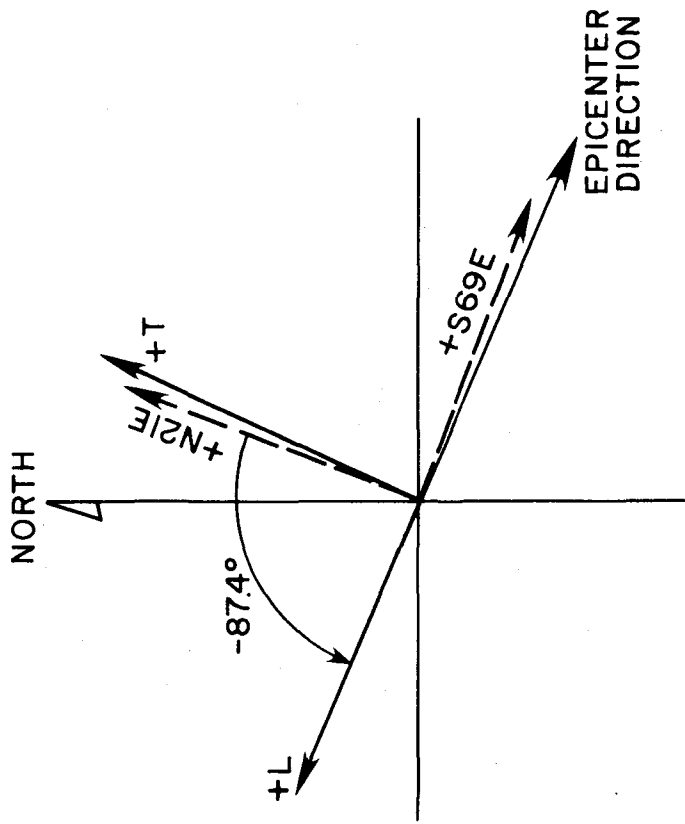


Fig. 5 Relation between components of seismograph and transformed coordinates (Kern County Earthquake)

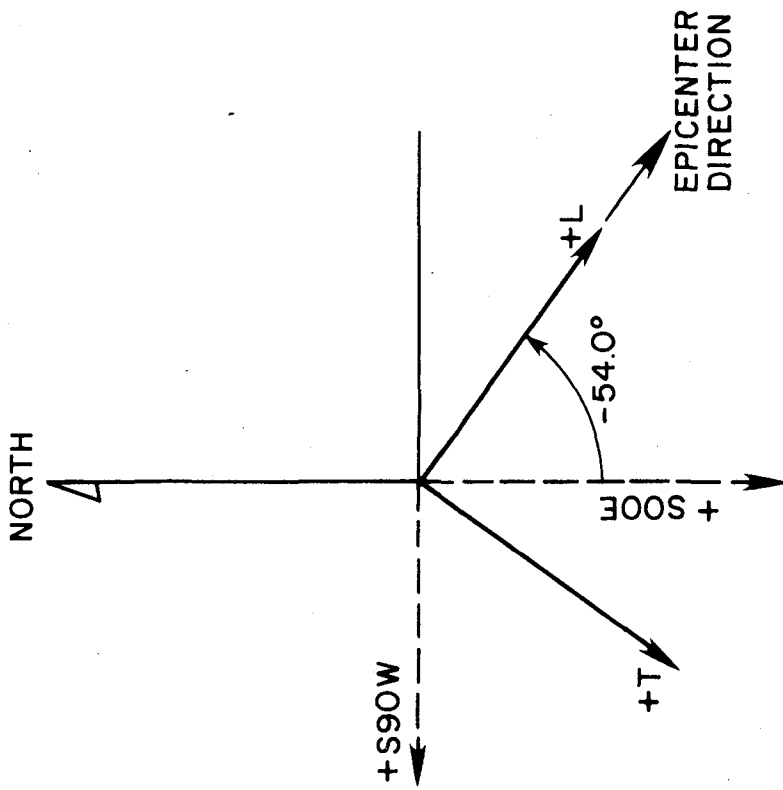


Fig. 4 Relation between components of seismograph and transformed coordinates (Imperial Valley Earthquake)

FL CENTRO 1940.5.18 IMPERIAL VALLEY

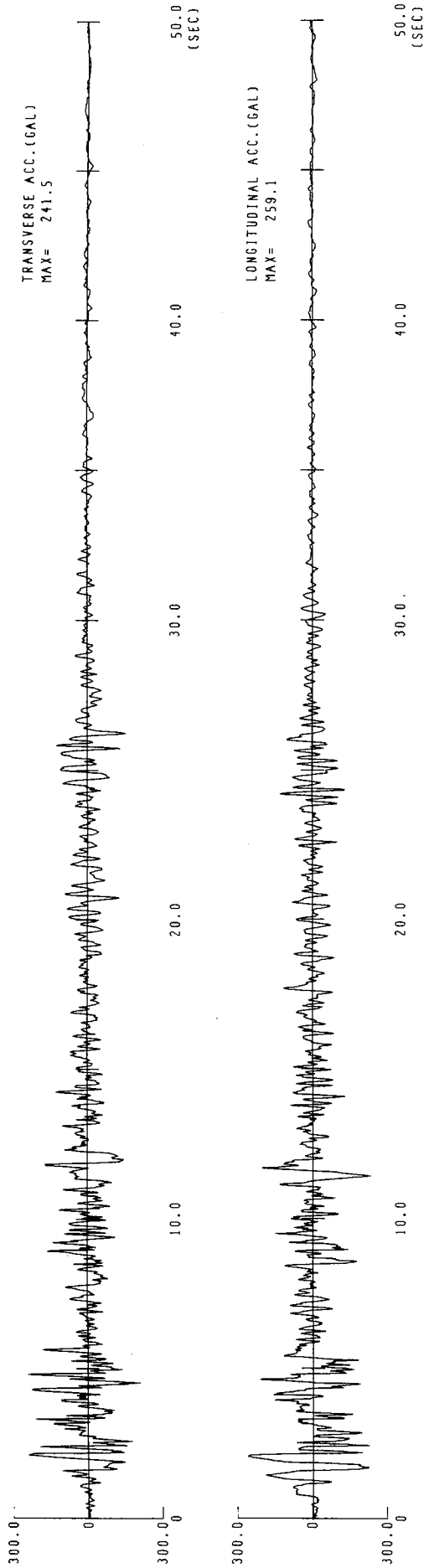


Fig. 6 Reproduced acceleration curves in longitudinal and transverse directions (Imperial Valley Earthquake)

FL CENTRO 1940.5.18 IMPERIAL VALLEY

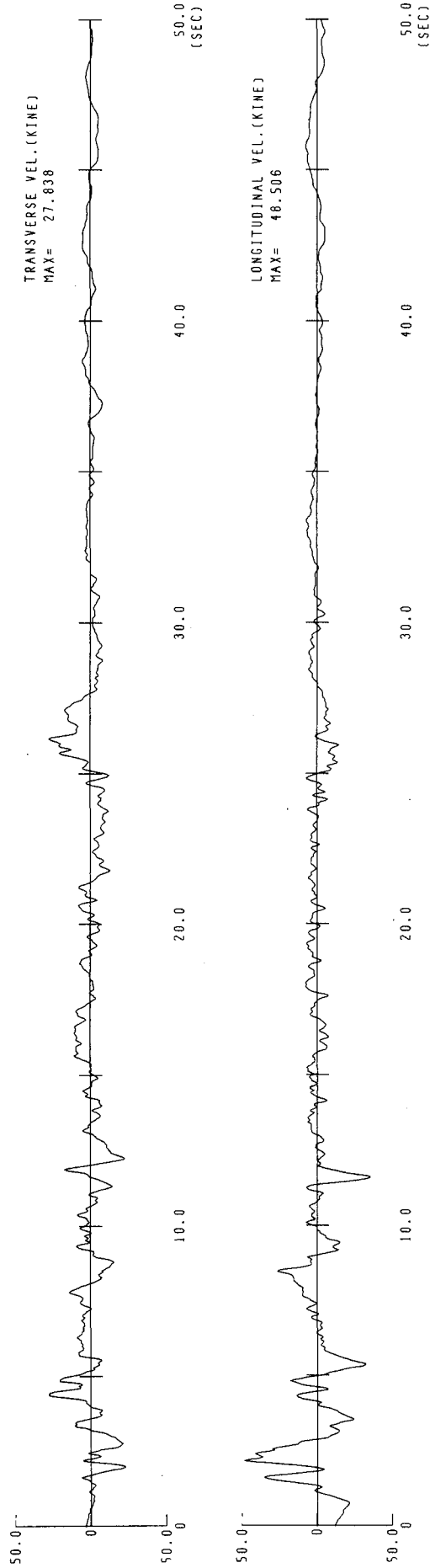


Fig. 7 Reproduced velocity curves in longitudinal and transverse directions (Imperial Valley Earthquake)

TAFT LINCOLN SCHOOL TUNNEL 1952.7.21 KERN COUNTY

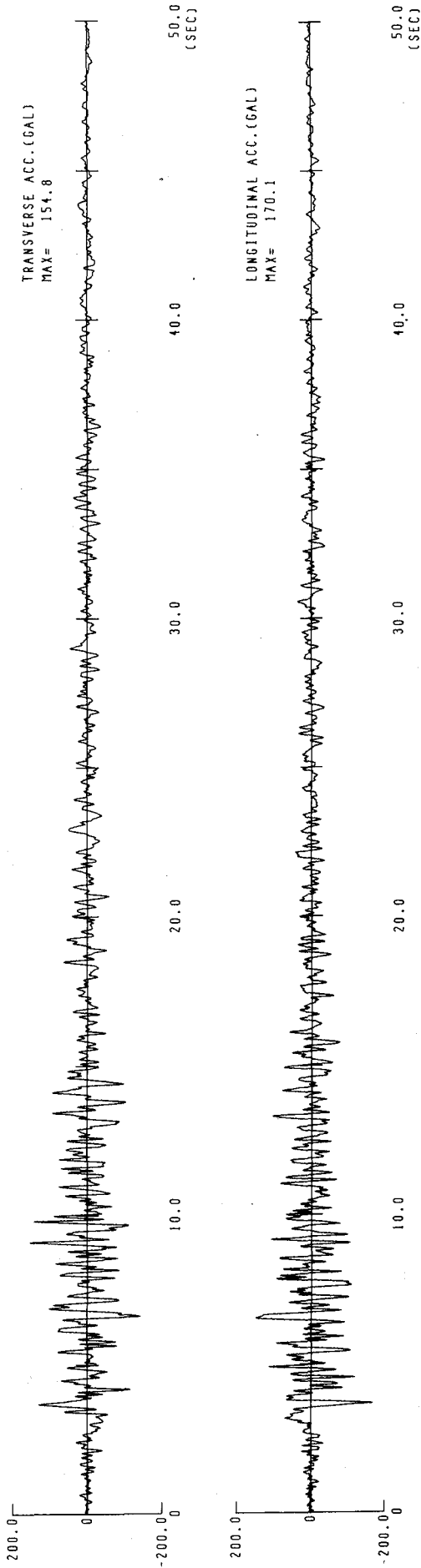


Fig. 8 Reproduced acceleration curves in longitudinal and transverse directions (Kern County Earthquake)

TAFT LINCOLN SCHOOL TUNNEL 1952.7.21 KERN COUNTY

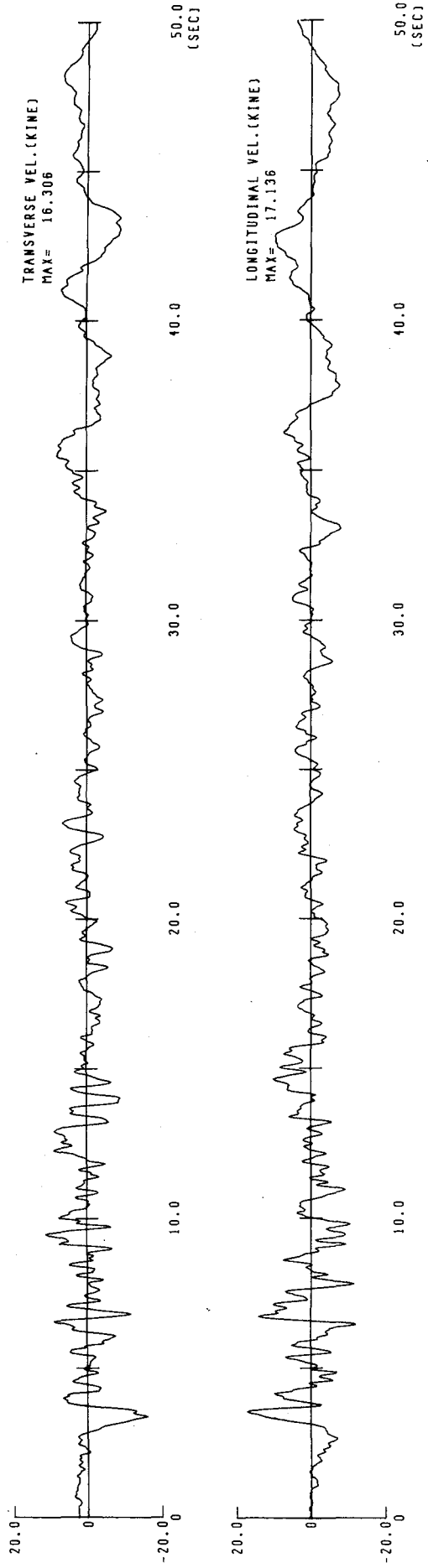


Fig. 9 Reproduced velocity curves in longitudinal and transverse directions (Kern County Earthquake)

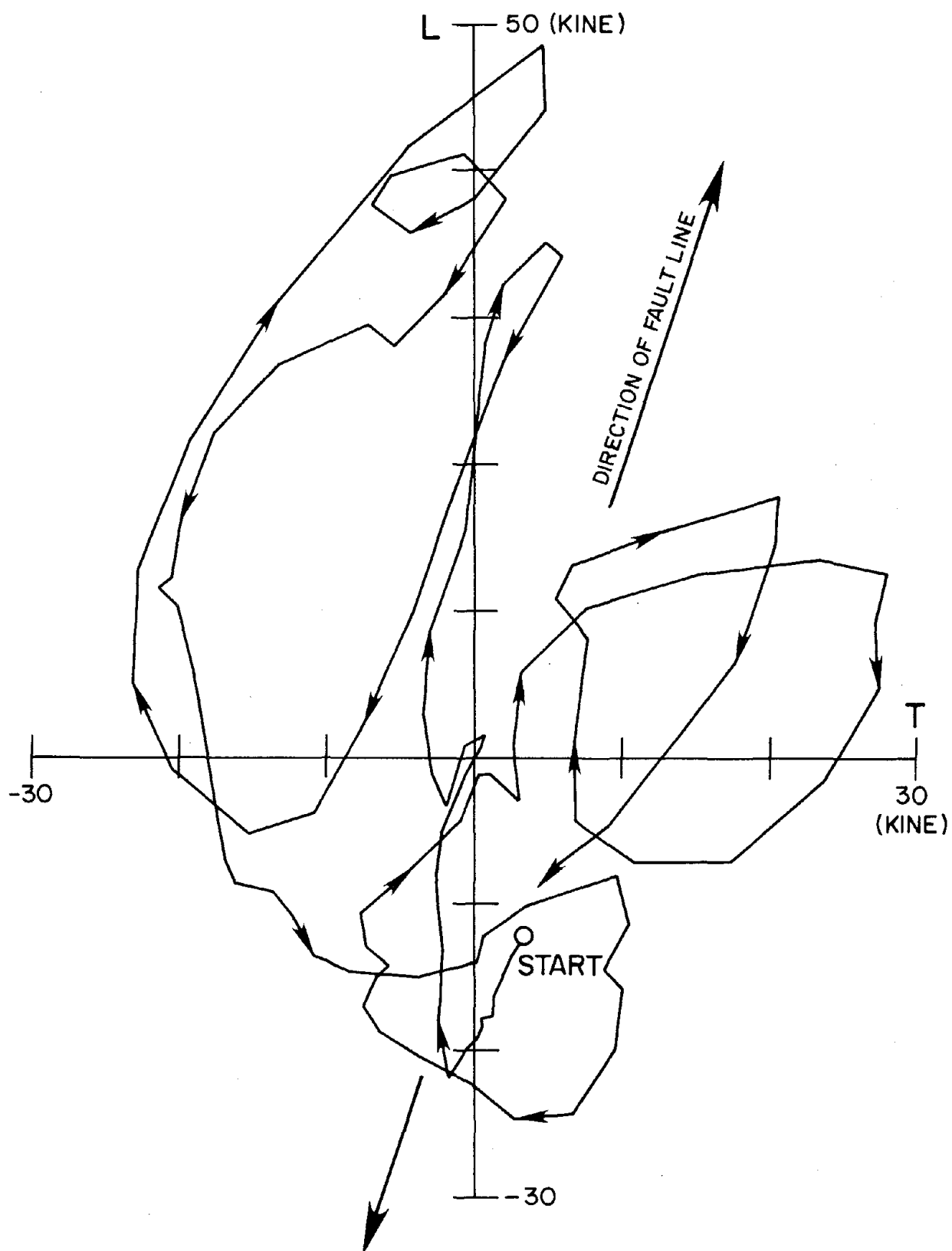


Fig. 10 Particle velocity orbit for first 6 seconds
at Imperial Valley Irrigation District

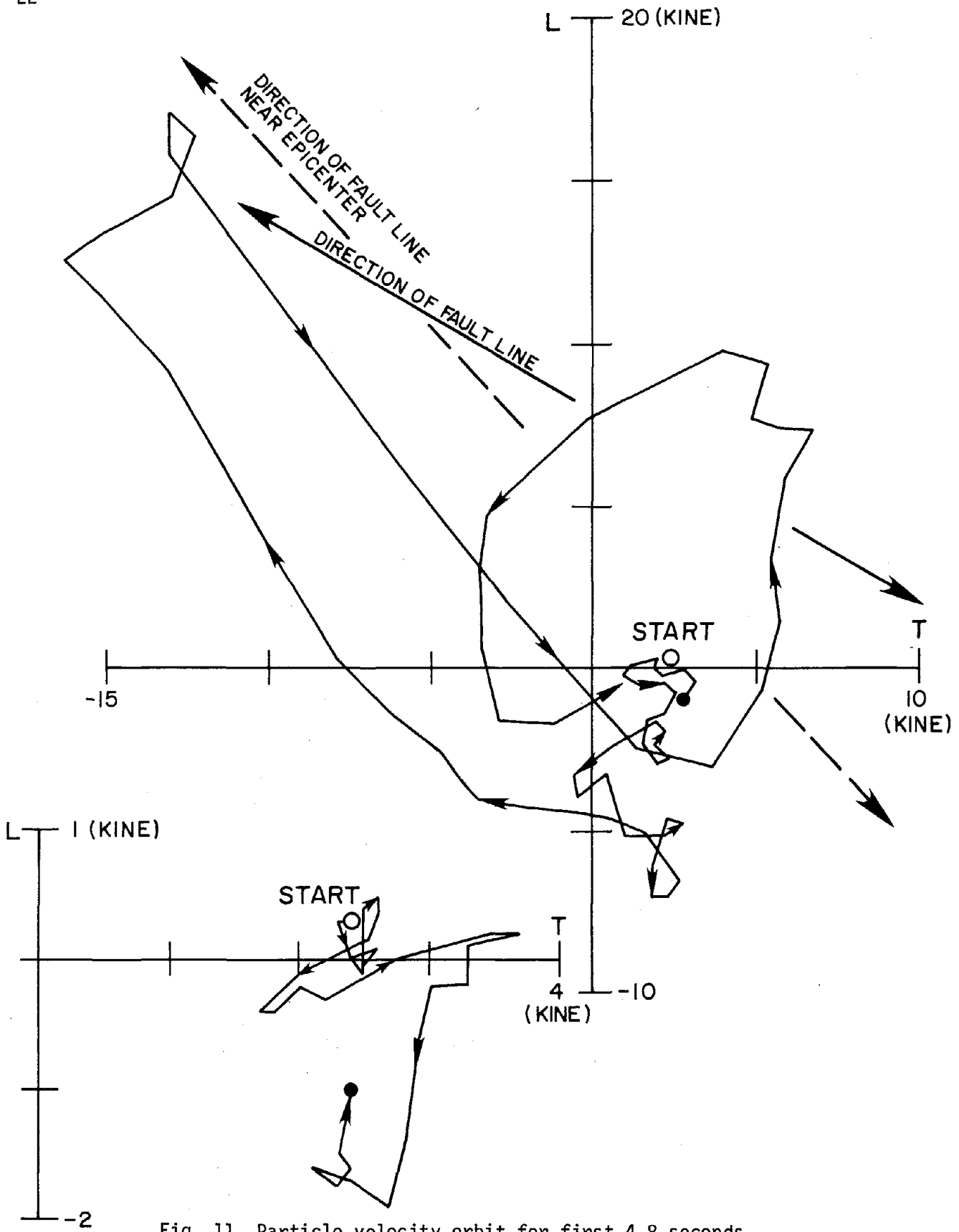


Fig. 11 Particle velocity orbit for first 4.8 seconds at Taft Lincoln School Tunnel

EL CENTRO 1940.5.18 IMPERIAL VALLEY

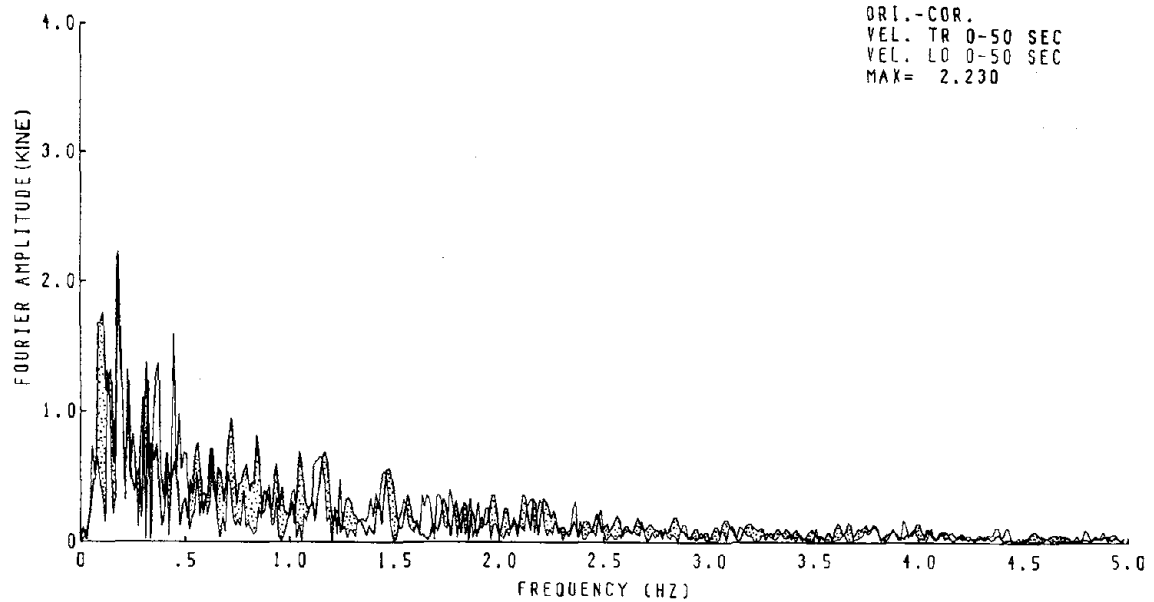


Fig. 12 Fourier amplitudes of longitudinal and transverse components relative to the direction from the epicenter - El Centro 0 - 50 sec.

EL CENTRO 1940.5.18 IMPERIAL VALLEY

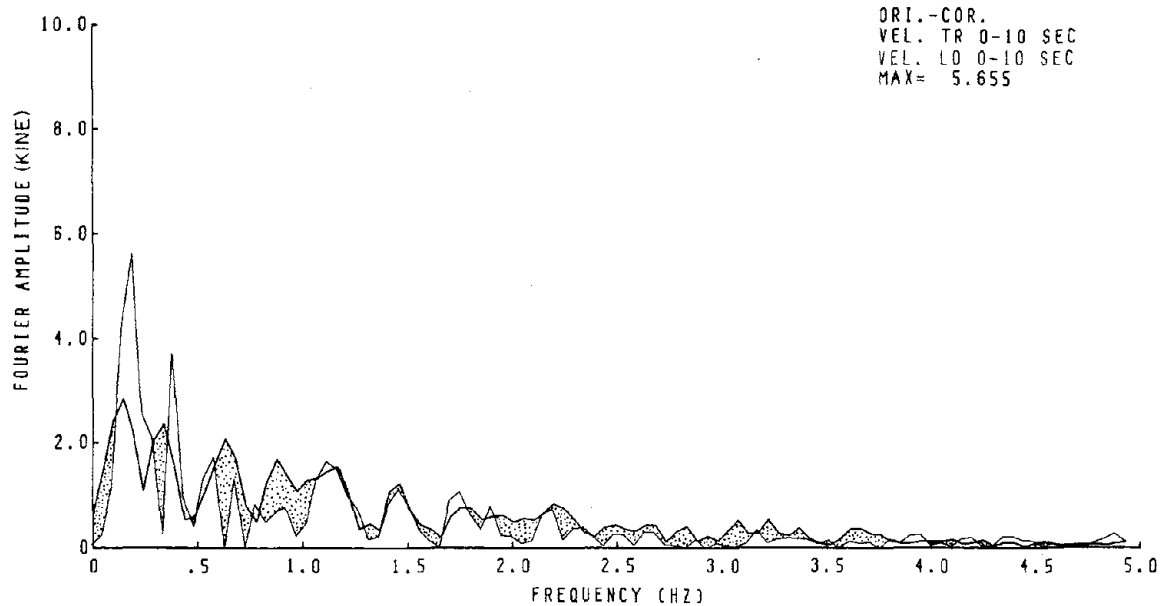


Fig. 13a Fourier amplitudes of longitudinal and transverse components relative to the direction from the epicenter - El Centro 0 - 10 sec.

EL CENTRO 1940.5.18 IMPERIAL VALLEY

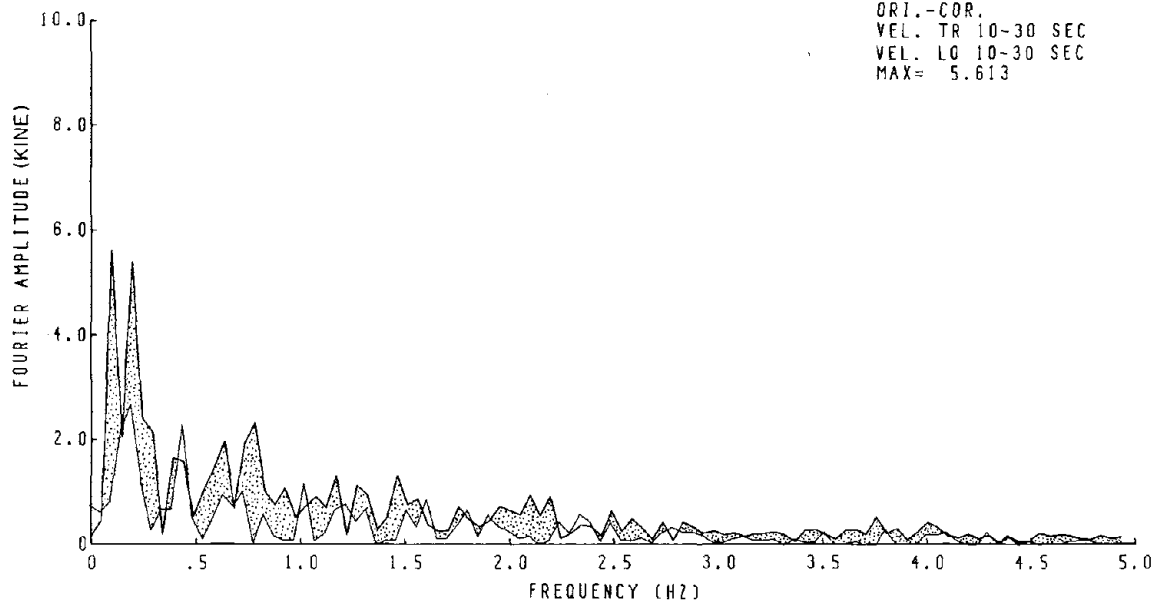


Fig. 13b Fourier amplitudes of longitudinal and transverse components relative to the direction from the epicenter - El Centro 10 - 30 sec.

EL CENTRO 1940.5.18 IMPERIAL VALLEY

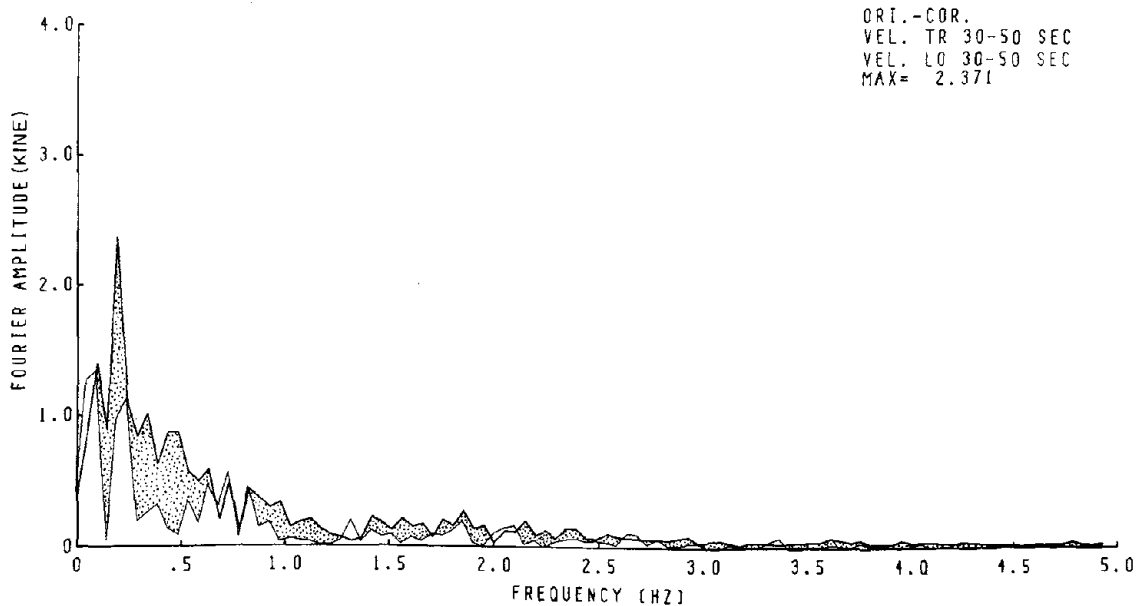


Fig. 13c Fourier amplitudes of longitudinal and transverse components relative to the direction from the epicenter - El Centro 30 - 50 sec.

TAFT LINCOLN SCHOOL TUNNEL 1952.7.21 KERN COUNTY

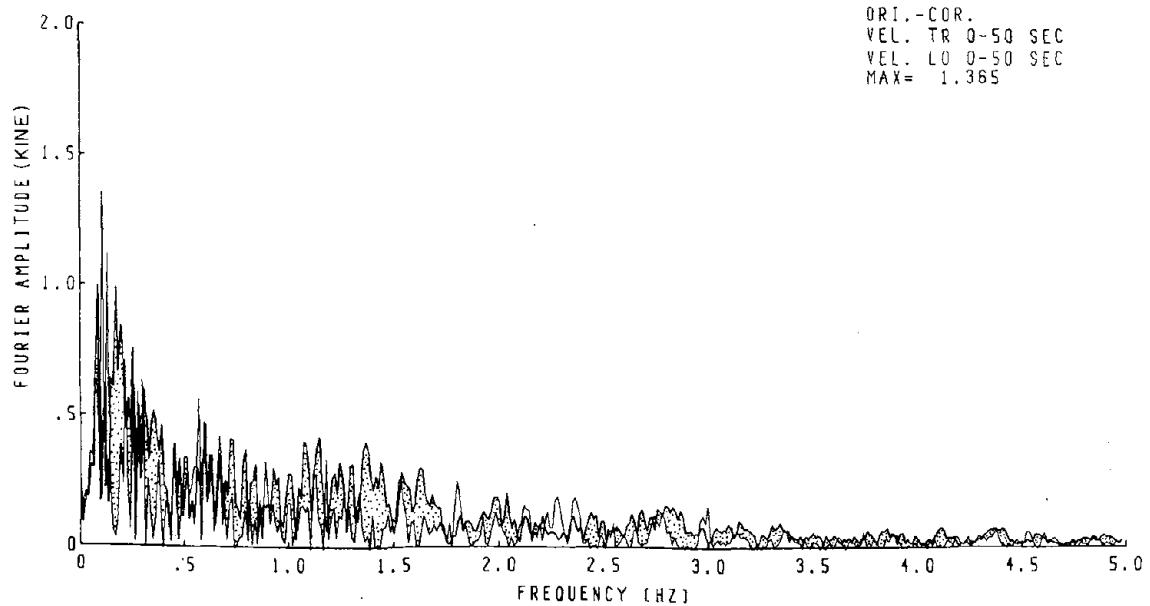


Fig. 14 Fourier amplitudes of transverse and corrected longitudinal components relative to the direction from the epicenter - Taft 0 - 50 sec.

TAFT LINCOLN SCHOOL TUNNEL 1952.7.21 KERN COUNTY

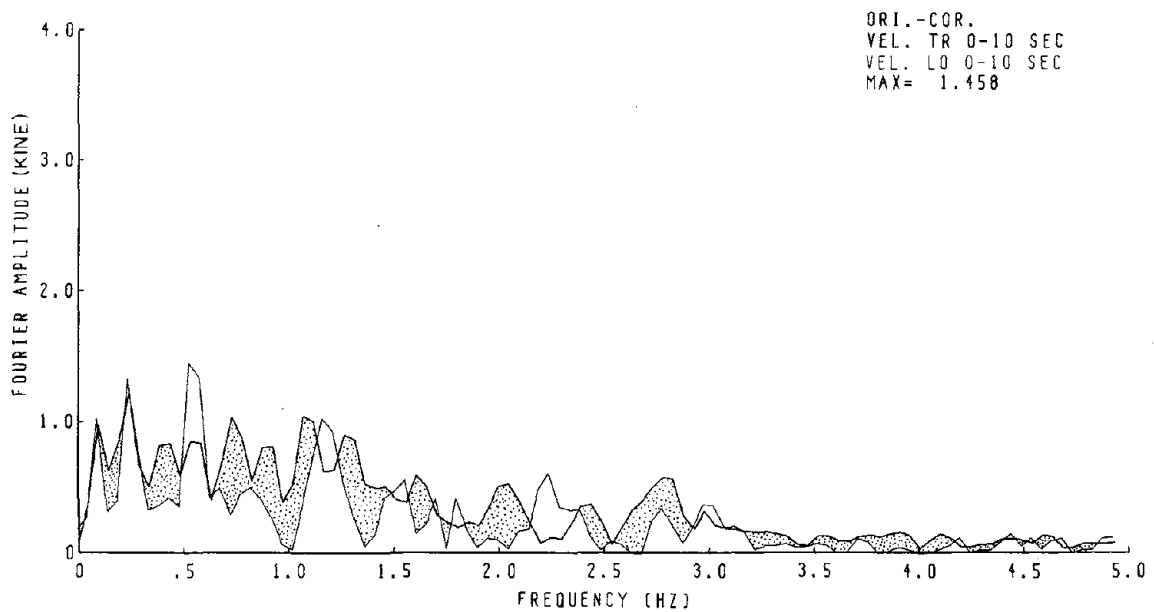


Fig. 15a Fourier amplitudes of transverse and corrected longitudinal components relative to the direction from the epicenter - Taft 0 - 10 sec.

TAFT LINCOLN SCHOOL TUNNEL 1952.7.21 KERN COUNTY

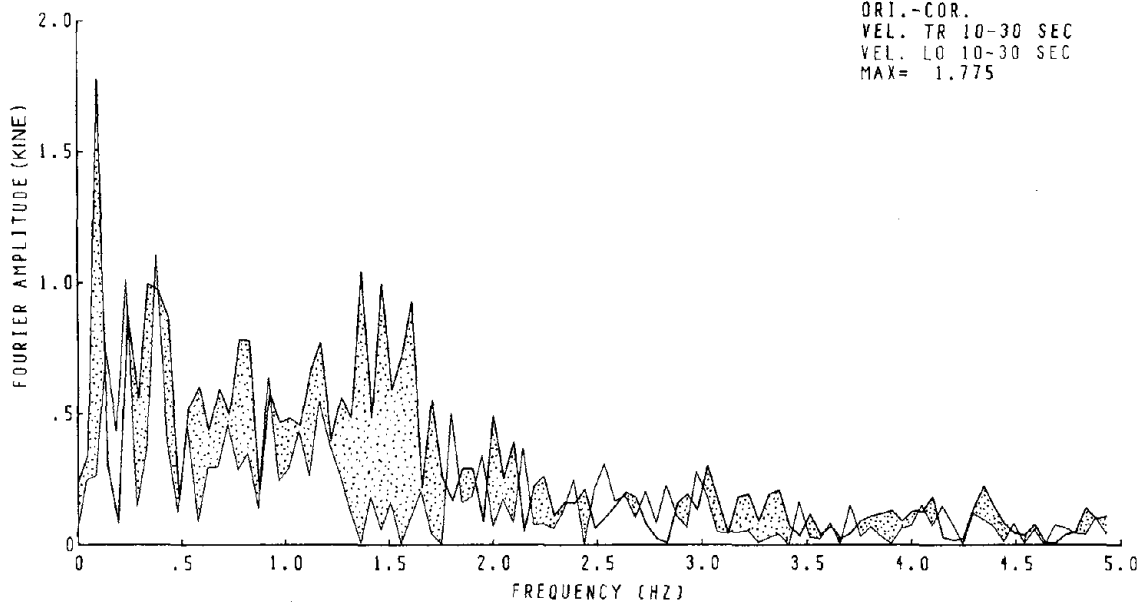


Fig. 15b Fourier amplitudes of transverse and corrected longitudinal components relative to the direction from the epicenter - Taft 10 - 30 sec.

TAFT LINCOLN SCHOOL TUNNEL 1952.7.21 KERN COUNTY

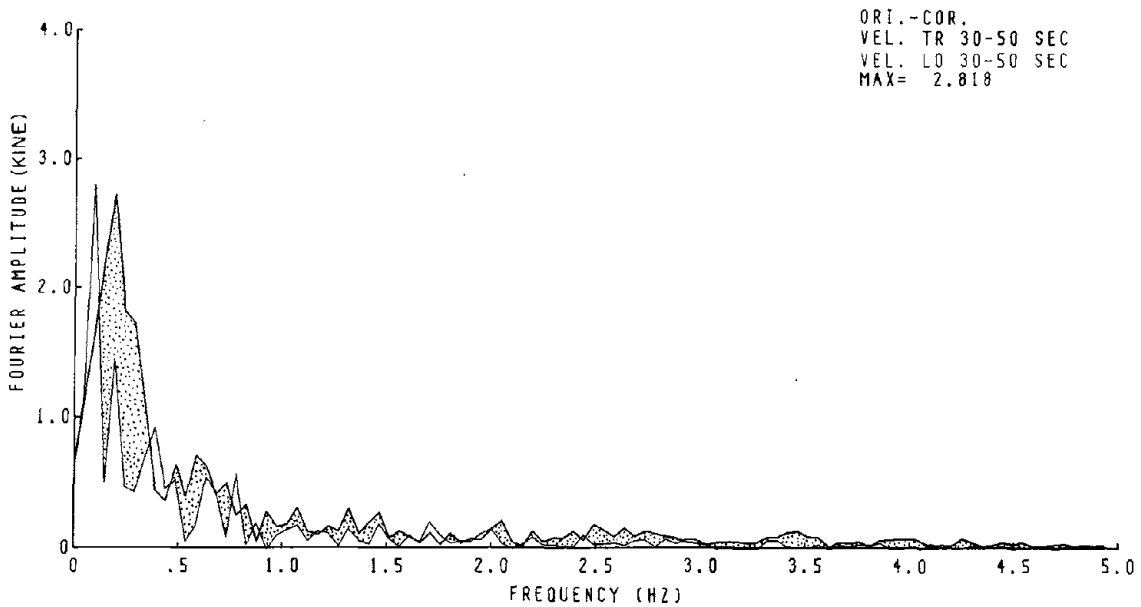


Fig. 15c Fourier amplitudes of transverse and corrected longitudinal components relative to the direction from the epicenter - Taft 30 - 50 sec.

EL CENTRO 1940.5.18 IMPERIAL VALLEY

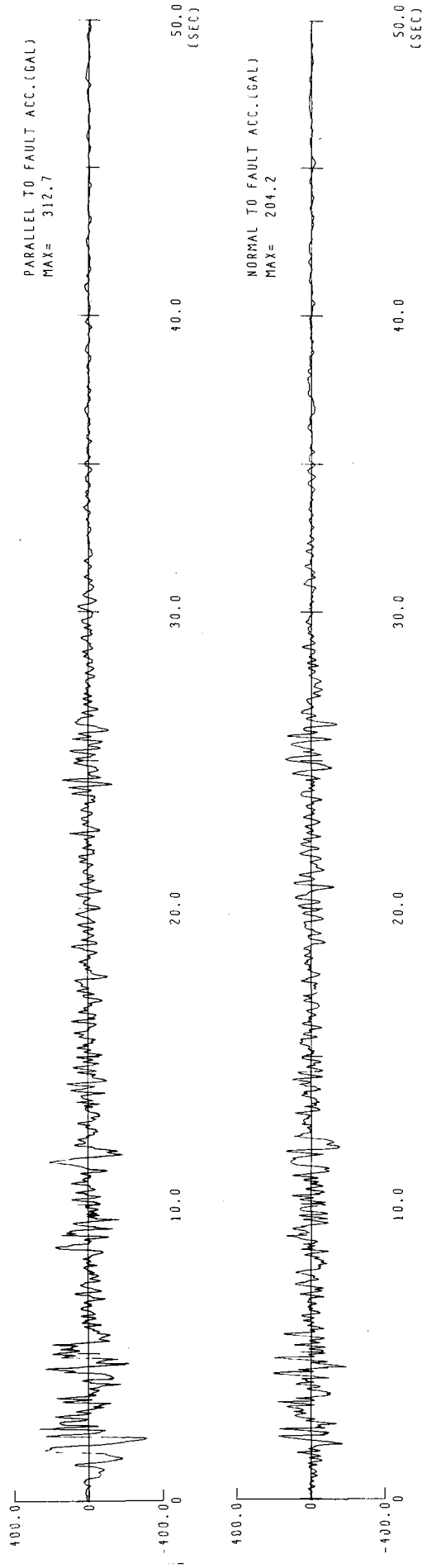


Fig. 16 Reproduced acceleration curves in normal and parallel directions (Imperial Valley Earthquake)

EL CENTRO 1940.5.18 IMPERIAL VALLEY

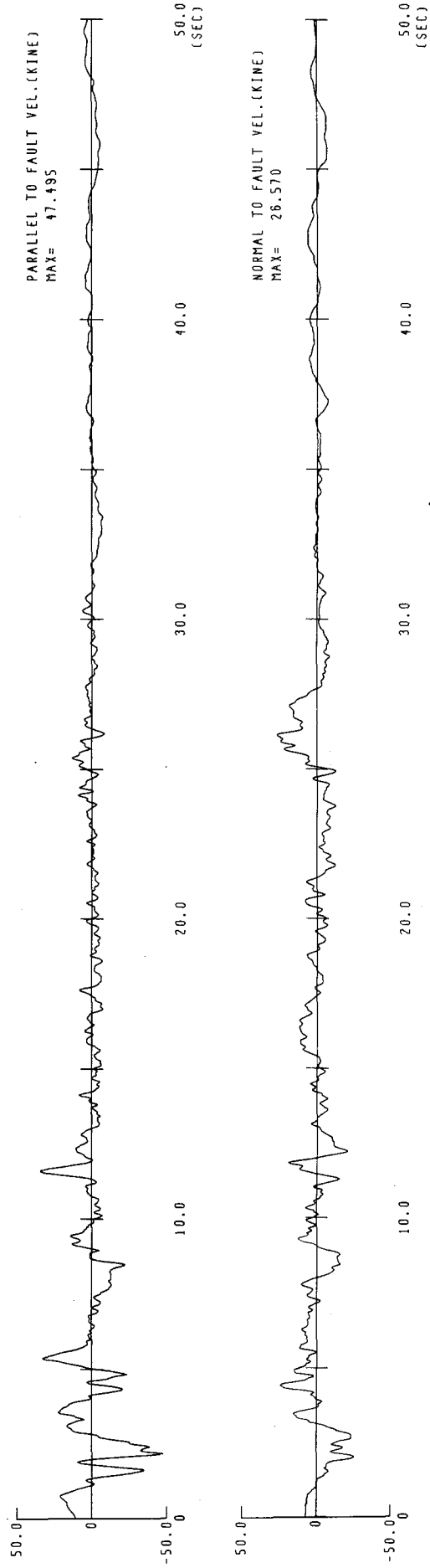


Fig. 17 Reproduced velocity curves in normal and parallel directions (Imperial Valley Earthquake)

TAFT LINCOLN SCHOOL TUNNEL 1952.7.21 KERN COUNTY

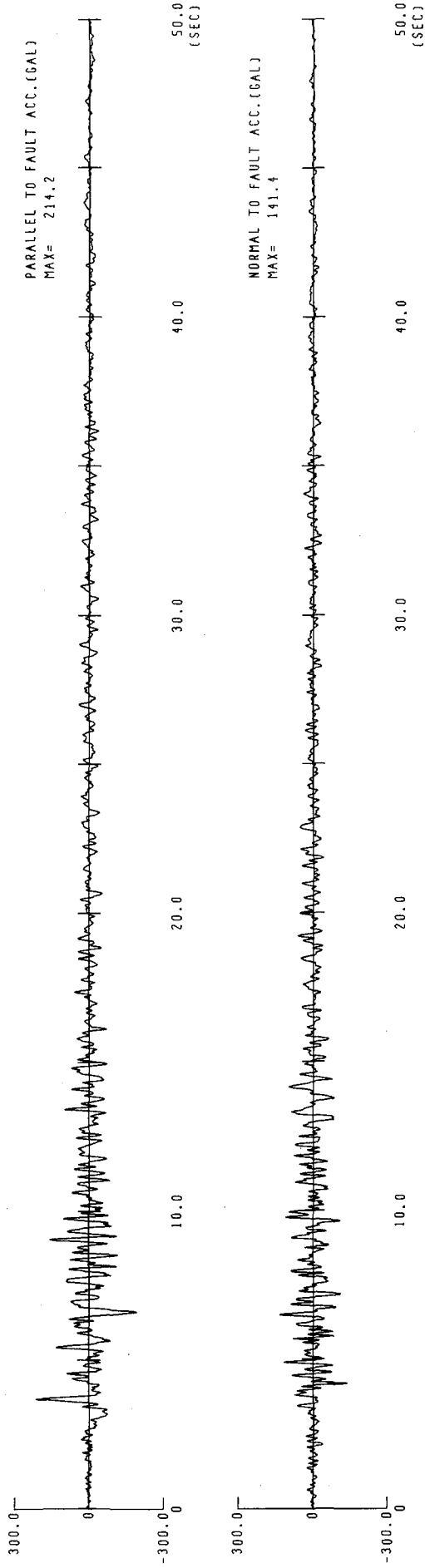


Fig. 18 Reproduced acceleration curves in normal and parallel directions (Kern County Earthquake)

TAFT LINCOLN SCHOOL TUNNEL 1952.7.21 KERN COUNTY

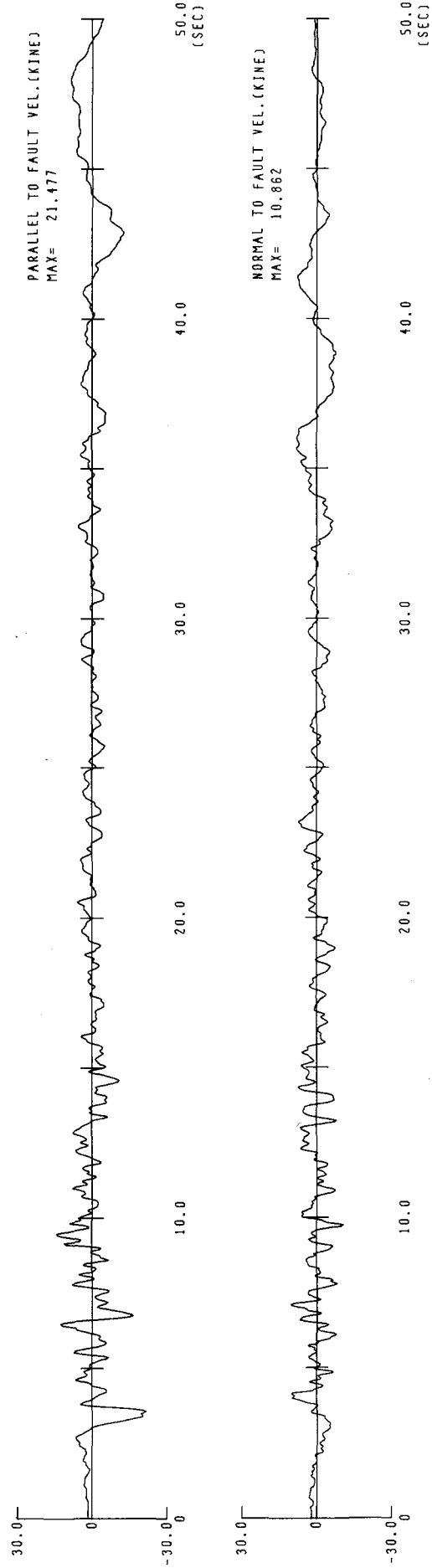


Fig. 19 Reproduced velocity curves in normal and parallel directions (Kern County Earthquake)

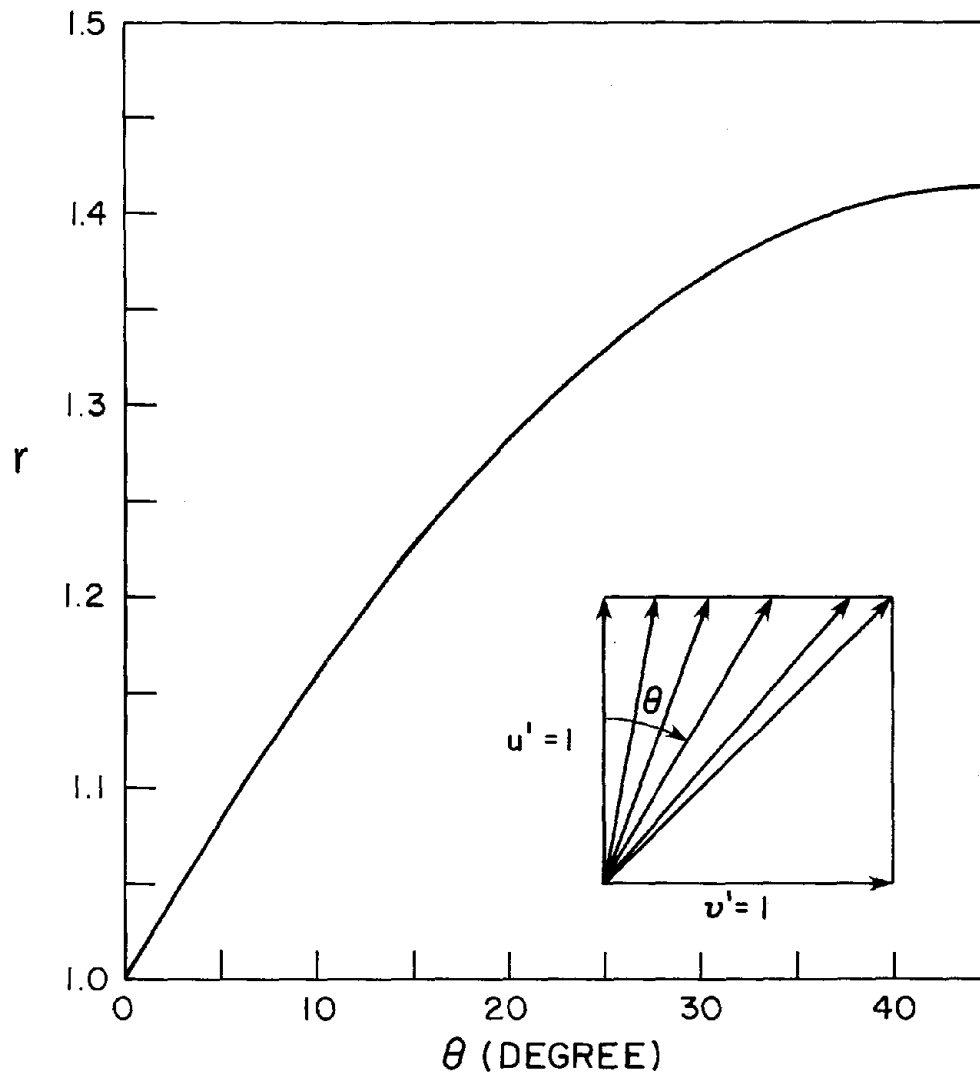


Fig. 20 Schematic explanation of coordinate transformation

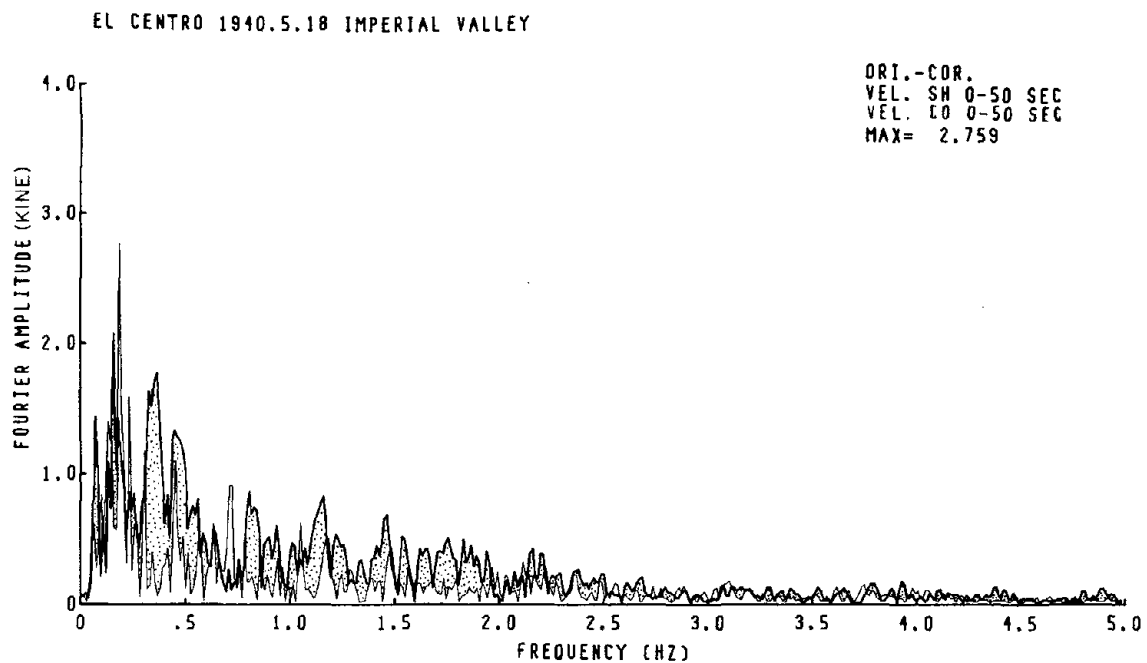


Fig. 21 Fourier amplitudes of parallel and corrected normal components in the direction of the fault line - El Centro 0 - 50 sec.

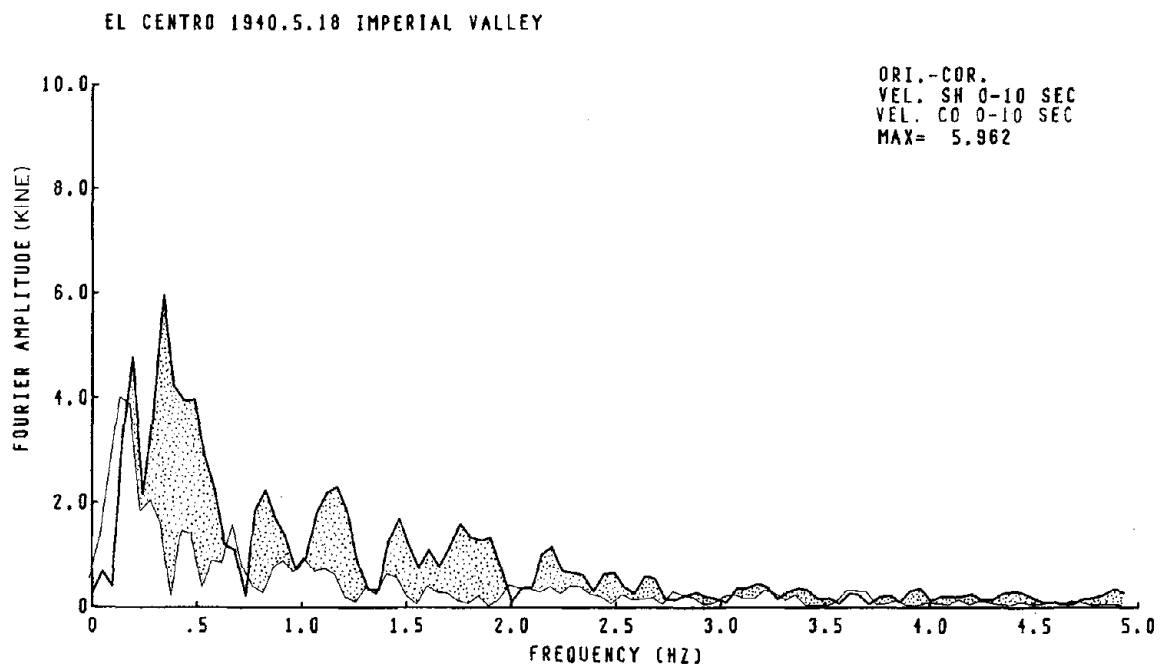


Fig. 22a Fourier amplitudes of parallel and corrected normal components in the direction of the fault line - El Centro 0 - 10 sec.

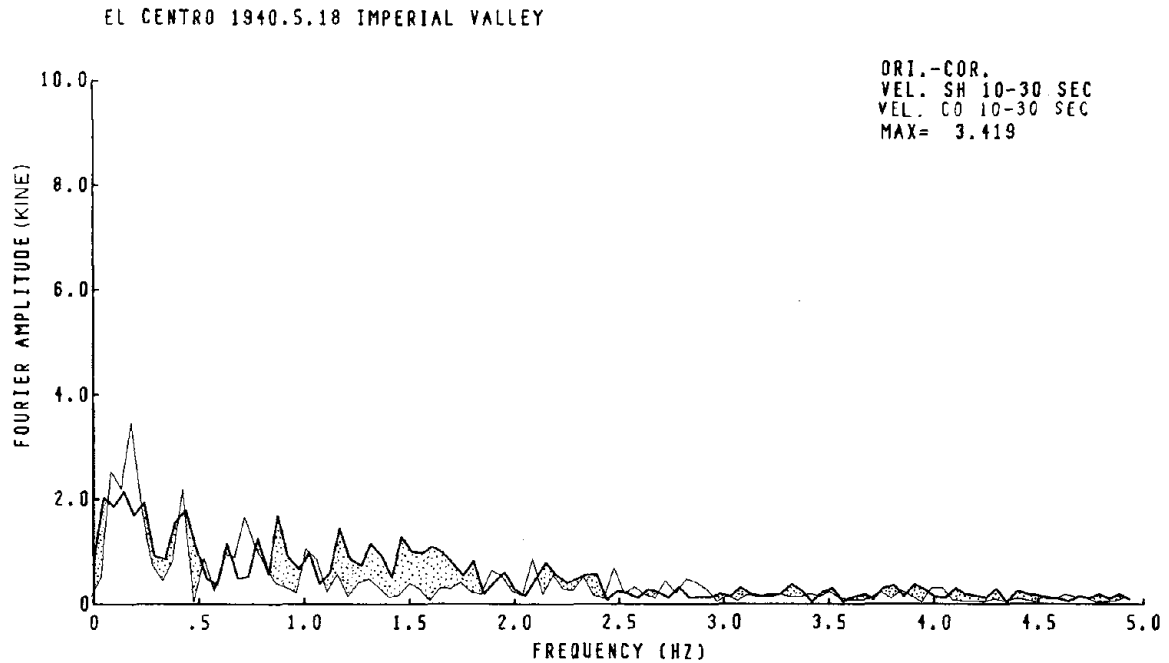


Fig. 22b Fourier amplitudes of parallel and corrected normal components in the direction of the fault line - El Centro 10 - 30 sec.

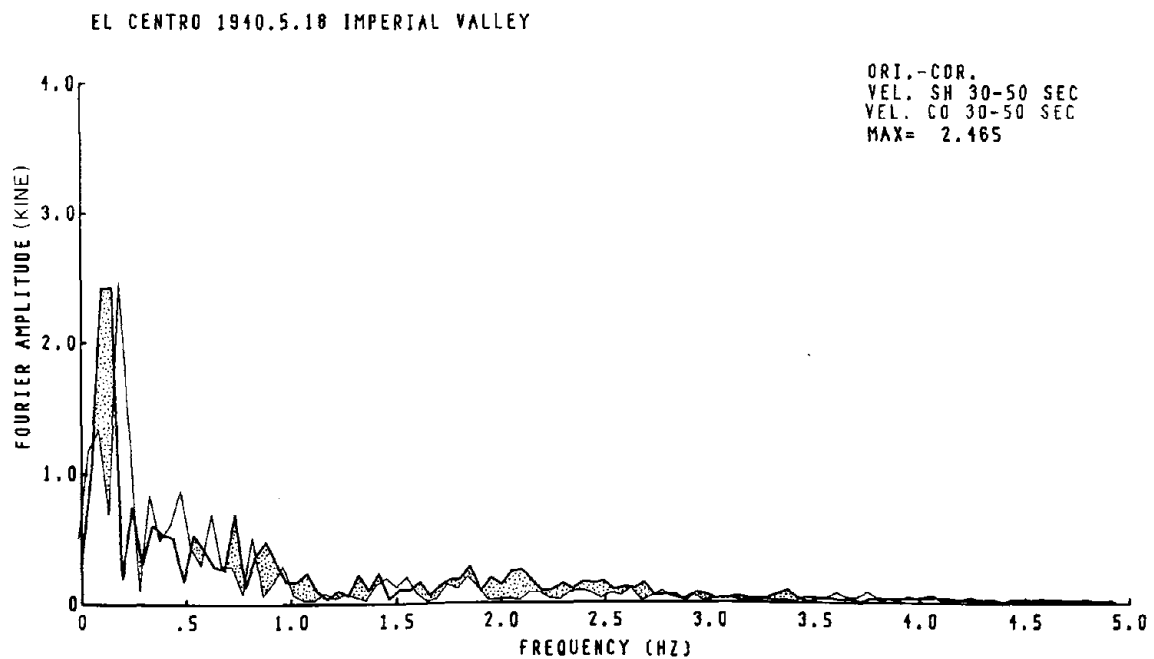


Fig. 22c Fourier amplitudes of parallel and corrected normal components in the direction of the fault line - El Centro 30 - 50 sec.

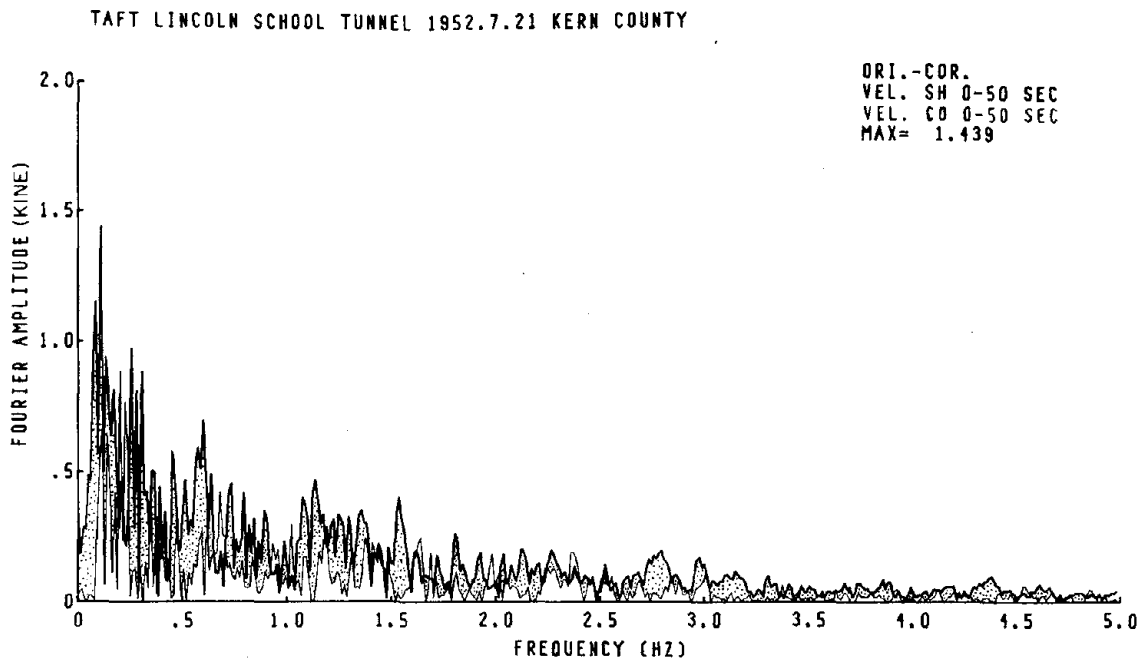


Fig. 23 Fourier amplitudes of parallel and corrected normal components in the direction of the fault line - Taft 0 - 50 sec.

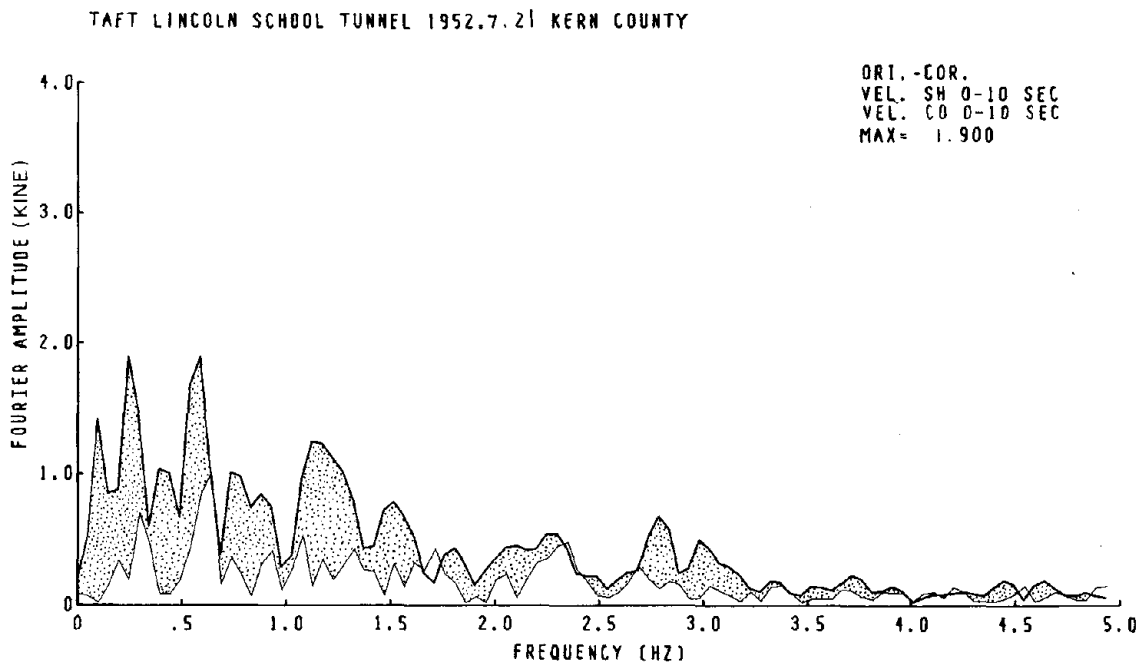


Fig. 24a Fourier amplitudes of parallel and corrected normal components in the direction of the fault line - Taft 0 - 10 sec.

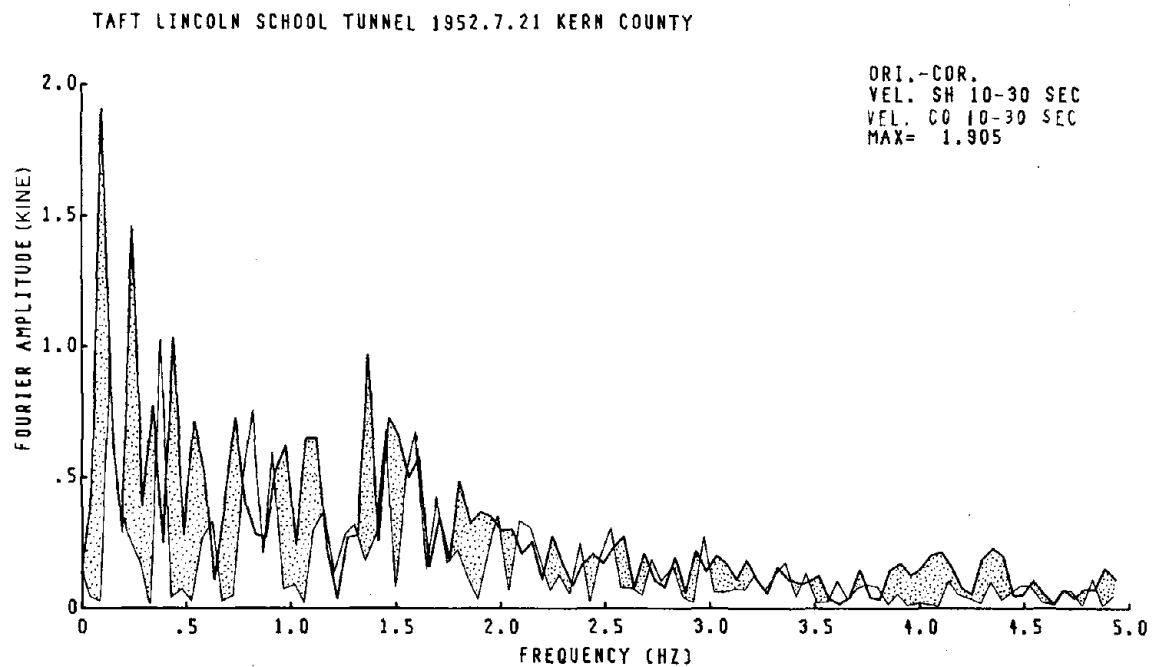


Fig. 24b Fourier amplitudes of parallel and corrected normal components in the direction of the fault line - Taft 10 - 30 sec.

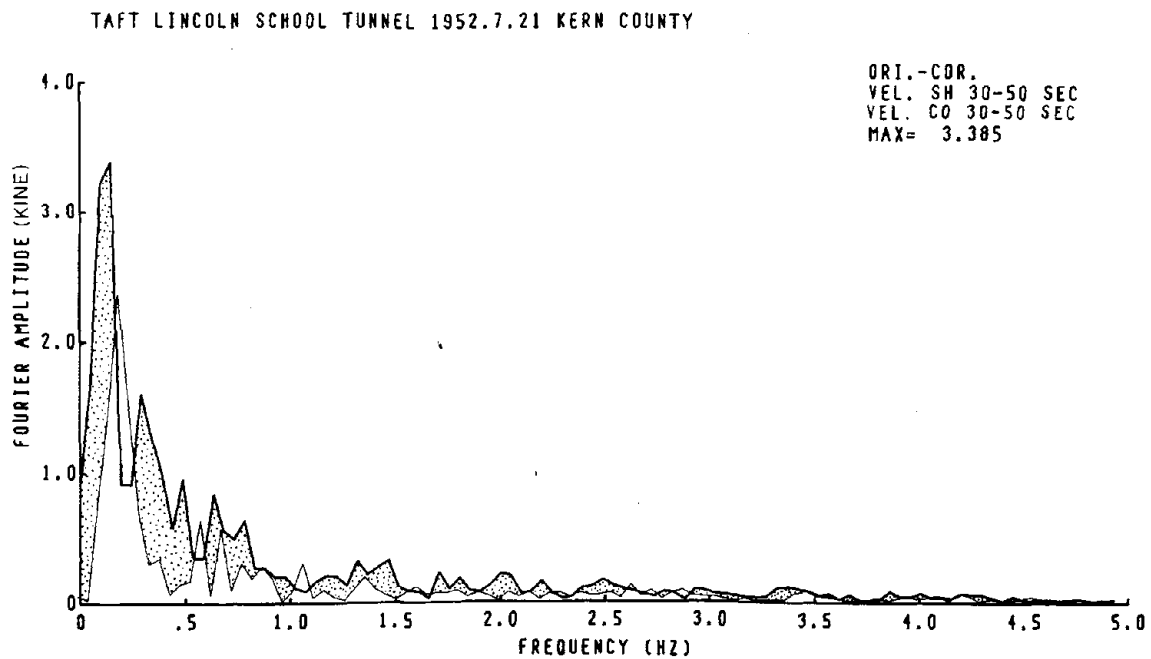


Fig. 24c Fourier amplitudes of parallel and corrected normal components in the direction of the fault line - Taft 30 - 50 sec.

Table 1 Properties of Earthquakes and Stations

	Example 1	Example 2
Name of earthquake	Imperial Valley, California	Kern County, California
Date and (local) time	May 18, 1940 20:37 PST	July 21, 1952 4:53 PDT
Epicenter location	32° 44' 00" N 115° 27' 00" W	35° 00' 00" N 119° 02' 00" W
Richter Magnitude	7.1	7.7
Approximate length of surface faulting (miles)	40 minimum	14
Number and name of station	117 El Centro, Imperial Valley Irrigation District	095 Taft, Lincoln School Tunnel
Station location	32° 47' 43" N 115° 32' 55" W	35° 09' 00" N 119° 27' 00" W
Site characteristics	Alluvium, more than 300 m	Alluvium
Structure type/size	2-story bldg.	1-story bldg.
Instrument location(s)	Ground level	Tunnel and roof
Components of instrument location	S00E S90E	N21E S69E
Modified Mercalli Intensity near station	VII to VIII	VII

Preceding page blank

Table 2 Subsurface Unit Thickness and Seismic Data at Each Station
(After Duke and Leeds, 1962)

Imperial Valley Irrigation District				
Thickness (feet)	V_p (fps)	Density (pcf)	$\frac{V_s}{V_p}$	V_s (fps)
100	522	128	1.0	522
1000	2810	139	1.0	2810
3000	3620	139	1.0	3620
3500	4050	147	1.0	4050
3500	7200	147	1.0	7200
	10000	172	1.0	10000

Taft Lincoln School				
Thickness (feet)	V_p (fps)	Density (pcf)	$\frac{V_s}{V_p}$	V_s (fps)
40	1190	140	0.45	535
160	5000	144	0.48	2399
500	6500	144	0.48	3119
3300	8000	148	0.48	3839
	15500	170	0.61	9454

Table 3 Maximum Value and Occurrence Time, Longitudinal and Transverse Components

Direction		Acceleration		Velocity	
		Max. Val (gal)	Occ. Time (sec)	Max. Val (kine)	Occ. Time (sec)
El Centro, Imperial Valley Irrigation District, May 18, 1940, Imperial Valley					
Longitudinal	S54E	259.1	2.08	48.5	2.16
Transverse	S36W	241.5	2.12	27.8	4.36
N-S	S00E	341.7	2.12	33.4	2.18
E-W	S90W	210.1	11.44	-36.9	2.14
Taft Lincoln School Tunnel, July 21, 1952, Kern County					
Longitudinal	N66.4W	-170.1	3.70	17.1	3.56
Transverse	N23.6E	154.8	9.10	-16.3	3.40
N-S	N21E	152.7	9.10	-15.7	3.40
E-W	S69E	175.9	3.70	-17.7	3.56

Table 4 Conditions of Computation and Corresponding Figure Number

Time (sec)	0 - 50	0 - 10	10 - 30	30 - 50
Number of data (n)	1251	251	501	501
Number used in FFT* (N)	2048	512	512	512
Frequency interval (Hz)	0.012	0.049	0.049	0.049
Nyquist frequency (Hz)	12.5	12.5	12.5	12.5
El Centro site	Fig. 12	Fig. 13a	Fig. 13b	Fig. 13c
Taft site	Fig. 14	Fig. 15a	Fig. 15b	Fig. 15c

*Remaining parts of data (N-n) are set to be equal to zero

Table 5 Peak Fourier Amplitude and
Frequency of Transverse Component at El Centro Site

0 - 50 sec.	0 - 10 sec.	10 - 30 sec.	30 - 50 sec.
0.11 (1.76)	----	0.10 (5.61)	0.10 (1.40)
0.18 (2.23)	0.15 (2.83)	1.20 (5.40)	0.20 (2.37)
0.32 (1.37)	0.34 (2.35)	----	0.34 (1.01)
0.72 (0.95)	----	----	0.73 (0.48)
0.84 (0.82)	0.88 (1.68)	----	0.83 (0.44)
1.17 (0.69)	1.17 (1.55)	1.17 (1.31)	----

Note: Numerals without parentheses are frequency (Hz) and those in parentheses are peak values of transverse components (kine)

Table 6 Peak Fourier Amplitude and
Frequency of Transverse Component at Taft Site

0 - 50 sec.	0 - 10 sec.	10 - 30 sec.	30 - 50 sec.
0.09 (1.00)	0.10 (0.97)	0.10 (1.78)	----
0.17 (0.99)	----	----	0.20 (2.72)
0.26 (0.76)	0.24 (1.22)	0.24 (0.88)	----
0.35 (0.52)	----	0.34 (1.00)	----
0.45 (0.39)	0.44 (0.83)	----	----
0.60 (0.47)	----	0.59 (0.60)	0.59 (0.71)
0.72 (0.41)	0.73 (1.03)	0.78 (0.78)	----
1.17 (0.42)	1.07 (1.04)	1.17 (0.77)	----
1.37 (0.40)	----	1.37 (1.04)	----

Note: Numerals without parentheses are frequency (Hz) and those in parentheses are peak values of transverse components (kine)

Table 7 Maximum Value and Occurrence Time, Normal and Parallel Components

Direction	Acceleration			Velocity		
	Max. Val (gal)	Occ. Time (sec)		Max. Val (kine)	Occ. Time (sec)	
El Centro, Imperial Valley Irrigation District, May 18, 1940, Imperial Valley						
Normal to fault	S54.5W	204.2	4.30	\ddot{u}	26.6	26.16
Parallel to fault	S35.5E	-312.7	2.12	\dot{v}	-47.5	2.16
N-S	S00E	341.7	2.12	\ddot{u}	33.4	2.18
E-W	S90W	210.1	11.44	\dot{v}	-36.9	2.14
Taft Lincoln School Tunnel, July 21, 1952, Kern County						
Normal to fault	N19.4W	-141.4	4.20	\ddot{u}	-10.9	9.76
Parallel to fault	N70.6E	214.2	3.70	\dot{v}	-21.5	3.56
N-S	N21E	152.7	9.10	\ddot{u}	-15.7	3.40
E-W	S69E	175.9	3.70	\dot{v}	-17.7	3.56

Table 8 Peak Fourier Amplitude and
Frequency of Parallel Component at El Centro Site

0 - 50 sec	0 - 10 sec.	10 - 30 sec.	30 - 50 sec.
0.07 (1.43)	----	----	0.10 (2.43)
0.18 (1.42)	0.20 (4.78)	0.24 (1.94)	0.24 (0.74)
0.37 (1.78)	0.34 (5.96)	----	0.34 (0.61)
0.45 (1.33)	0.49 (3.97)	0.44 (1.79)	----
0.81 (0.87)	0.83 (2.24)	0.88 (1.68)	0.88 (0.48)
1.16 (0.83)	1.17 (2.30)	1.17 (1.44)	----
1.47 (0.69)	1.47 (1.70)	1.47 (1.28)	----
1.54 (0.52)	1.61 (1.09)	1.61 (1.10)	----
1.76 (0.52)	1.76 (1.60)	----	----
1.83 (0.50)	1.90 (1.33)	1.81 (0.83)	----

Note: Numerals without parentheses are frequency (Hz) and those in parentheses are peak values of parallel components (kine)

Table 9 Peak Fourier Amplitude and
Frequency of Parallel Component at Taft Site

0 - 50 sec.	0 - 10 sec.	10 - 30 sec.	30 - 50 sec.
0.11 (1.44)	0.10 (1.42)	0.10 (1.91)	0.15 (3.39)
0.26 (0.97)	0.24 (1.90)	0.24 (1.46)	----
0.31 (0.88)	----	----	0.29 (1.60)
0.45 (0.58)	0.39 (1.40)	0.44 (1.03)	0.49 (0.95)
0.60 (0.70)	0.59 (1.90)	----	0.64 (0.84)
0.73 (0.45)	0.73 (1.01)	0.73 (0.73)	0.78 (0.64)
1.14 (0.47)	1.12 (1.25)	1.07 (0.65)	----
1.54 (0.40)	1.51 (0.78)	----	----

Note: Numerals without parentheses are frequency (Hz) and those in parentheses are peak values of parallel components (kine)

Table 10 Simplified Seismic Data at El Centro Site

Case	Depth (ft)	\bar{V}_s (fps)	\bar{f} (Hz)
1	100	522	1.31
2	1100	2602	0.59
3	4100	3347	0.20
4	7600	3671	0.12
5	11100	4784	0.11

Table 11 Simplified Seismic Data at Taft Site

Case	Depth (ft)	\bar{V}_s (fps)	\bar{f} (Hz)
1	40	535	3.34
2	200	2026	2.53
3	700	2807	1.00
4	4000	3658	0.23

Table 12 Estimated Lower and Upper Limit of Shear Strain at El Centro Site

Fourier Amplitude		Shear Strain $\times 10^{-3}$ (%)			
f (Hz)	Amp (kine)	\bar{f} (Hz)	Lower Limit	\bar{f} (Hz)	Upper Limit
0.07	1.43	--	--	0.11	0.98
0.18	1.42	0.12	1.27	0.20	1.40
0.37	1.78	0.20	1.75	0.59	2.25
0.45	1.33	0.20	1.31	0.59	1.68
0.81	0.87	0.59	1.10	1.31	5.48
1.16	0.83	0.59	1.05	1.31	5.23
1.47	0.69	1.31	4.35	--	--
1.54	0.52	1.31	3.28	--	--
1.76	0.52	1.31	3.28	--	--
1.83	0.50	1.31	3.15	--	--

Table 13 Estimated Lower and Upper Limit of Shear Strain at Taft Site

Fourier Amplitude		Shear Strain $\times 10^{-4}$ (%)			
f (Hz)	Amp (kine)	\bar{f} (Hz)	Lower Limit	\bar{f} (Hz)	Upper Limit
0.11	1.44	--	--	0.23	12.95
0.26	0.97	0.23	8.72	1.00	11.37
0.31	0.88	0.23	7.91	1.00	10.31
0.45	0.58	0.23	5.22	1.00	6.80
0.60	0.70	0.23	6.29	1.00	8.20
0.73	0.45	0.23	4.05	1.00	5.27
1.14	0.47	1.00	5.51	2.53	7.63
1.54	0.40	1.00	4.69	2.53	6.49

REFERENCES

1. Ohsaki, Y., "The Effects of Local Soil Conditions upon Earthquake Damage," Soil Dynamics, Proc. of Specialty Session 2, 7th ICSMFE, Mexico, 1969
2. Seed, H. B., "The Influence of Local Soil Conditions on Earthquake Damage," Soil Dynamics, Proc. of Specialty Session 2, 7th ICSMFE, Mexico, 1969
3. Hardin, B. O. and Drnevich, V. P., "Shear Modulus and Damping in Soils, I - Measurement and Parameter Effects," Technical Report UKY 26-70-CE2, University of Kentucky, 1970
4. Hardin, B. O. and Drnevich, V. P., "Shear Modulus and Damping in Soils, II - Design Equations and Curves," Technical Report UKY 27-70-CE3, University of Kentucky, 1970
5. Richart, F. E., Jr., Hall, J. R., Jr., and Woods, R. D., "Vibrations of Soils and Foundations," Prentice-Hall, 1970
6. Seed, H. B. and Idriss, I. M., "Soil Moduli and Damping Factors for Dynamic Response Analyses," Report No. EERC 70-10, Earthquake Engineering Research Center, University of California, Berkeley, California, 1970
7. Seed, H. B., Ugas, C. and Lysmer, J., "Site-Dependent Spectra for Earthquake-Resistant Design," Report No. EERC 74-12, Earthquake Engineering Research Center, University of California, Berkeley, California, 1974
8. Seed, H. B., Whitman, R. V., Dezfulian, H., Dorby, R. and Idriss, I. M., "Relationships between Soil Conditions and Building Damage in the 1967 Caracas Earthquake," Journal of the Soil Mechanics and Foundations Division, ASCE, 1972
9. California Institute of Technology, Earthquake Engineering Research Laboratory, "Strong Motion Earthquake Accelerograms, Digitized and Plotted Data," Volume I - Uncorrected Accelerograms, Part A, Report of Earthquake Engineering Research Laboratory, EERL 70-20, California Institute of Technology, Pasadena, California, 1969
10. Trifunac, M. D., "Low Frequency Digitization Errors and a New Method for Zero Base-Line Correction of Strong-Motion Accelerograms," Report of Earthquake Engineering Research Laboratory, EERL 70-07, California Institute of Technology, Pasadena, California, 1970
11. Trifunac, M. D., Udawadia, F. E. and Brady, A. G., "High Frequency Errors and Instrument Corrections of Strong-Motion Accelerograms," Report of Earthquake Engineering Research Laboratory, EERL 71-05, California Institute of Technology, Pasadena, California, 1971

Preceding page blank

12. California Institute of Technology, Earthquake Engineering Research Laboratory, "Strong Motion Earthquake Accelerograms, Digitized and Plotted Data," Volume II - Corrected Accelerograms and Integrated Ground Velocity and Displacement Curves, Part A, Report of Earthquake Engineering Research Laboratory, EERL 71-50, California Institute of Technology, Pasadena, California, 1971
13. Hudson, D. E., Preface to the Series in "Strong-Motion Earthquake Accelerograms Digitized and Plotted Data," Volume II - Corrected Accelerograms and Integrated Ground Velocity and Displacement Curves, Part A, Report of Earthquake Engineering Research Laboratory, EERL 71-50, California Institute of Technology, Pasadena, California, 1971
14. Duke, C. M. and Leeds, D. J., "Site Characteristics of Southern California Strong-Motion Earthquake Stations," Report No. 62-55, Department of Engineering, University of California, Los Angeles, California, November 1962
15. Hansen, W. R., Weiss, R. B., Idriss, I. M. and Cluff, L. S., "Geotechnical Data Compilations for Selected Strong-Motion Seismograph Sites in California," prepared for National Oceanic and Atmospheric Administration, Woodward-Lundgren & Associates, Consulting Engineers and Geologists, Oakland, California, December 1973
16. United States Department of the Interior, Geological Survey, "Strong-Motion Accelerograph Station List - 1975," Open File Report No. 76-79, March 1976
17. State of California, The Resources Agency, Department of Conservation, "Geologic Map of California, San Diego - El Centro Sheet," Compilation by R. G. Strand, 1962, Second Printing, 1973
18. State of California, The Resources Agency, Department of Conservation, "Geologic Map of California, Bakersfield Sheet," Compilation by A. R. Smith, 1964
19. Richter, C. F., "Elementary Seismology," W. H. Freeman and Company, 1958
20. Bonilla, M. G., "Surface Faulting and Related Effects," in "Earthquake Engineering," edited by R. L. Wiegel, Chapter 3, Prentice-Hall, 1970
21. Coffman, J. L. and von Hake, C. A., "Earthquake History of the United States," Publication 41-1, Revised Edition, U.S. Department of Commerce, National Oceanic and Atmospheric Administration, 1973
22. Cooley, J. W. and Tukey, J. W., "An Algorithm for the Machine Calculation of Complex Fourier Series," Mathematics of Computation, Vol. 19, No. 90, pp. 297-301, The American Mathematical Society, 1965

23. Kubo, T. and Penzien, J., "Time and Frequency Domain Analyses of Three Dimensional Ground Motions, San Fernando Earthquake," Report No. EERC 76-6, Earthquake Engineering Research Center, University of California, Berkeley, California, 1976

APPENDIX

Computer Program Listings

Preceding page blank

```

PROGRAM CORIN(INPUT,OUTPUT,TAPE1,TAPES=INPUT,TAPE6=OUTPUT,PUNCH)
COMMON /DATAN/X(2501,2),XD(2500,2),XMAX(2,2)
COMMON /N11/NAME(8)
CORRECTION OF ORIGINAL TWO HORIZONTAL DIRECTION DATA INTO
LONGITUDINAL AND TRANSVERSE COMPONENTS TOWARD THE EPICENTER
INPUT DATA
NAME = NAME OF EARTHQUAKE
TT = DURATION (SEC) AND TT.LE.50.0
TETA = ANGLE OF N TO L OR E TO T
      +=CLOCKWISE, -=COUNTERCLOCKWISE
IND1 = NE.0 IF PRINT OUT DATA ARE NECESSARY
IND2 = NE.0 IF PUNCH OUT DATA ARE NECESSARY
IND3 = NE.0 IF PLOT OUT DATA ARE NECESSARY
CAUTION - ORIGINAL DATA SHOULD BE AS A RIGHTHAND SYSTEM, I.E.,
          IF N SIDE IS POSITIVE, E SIDE SHOULD BE POSITIVE,
          IF S SIDE IS POSITIVE, W SIDE SHOULD BE POSITIVE.
READ(5,40) NAME
READ(5,100) TT
READ(5,100) TETA
READ(5,101) IND1,IND2,IND3
NA=FIX(TT/0.02)+1
NV=NA/2+1
CALL SETFXB(5LTAPE1,2500,100)
CALL INPUT(NA)
TETA = TETA *0.0174533
XMAX1=0.0
XMAX2=0.0
X1=COS(TETA)
X2=SIN(TETA)
DO 901 K=1,NA
  XX=X(K,1)
  XY=X(K,2)
  XK1=XX*XX1+XY*XY2
  XK2=XY*XX1-XX*XY2
  XMAX1=AMAX1(XMAX1,ABS(XK1))
  XMAX2=AMAX1(XMAX2,ABS(XK2))
  X(K,1)=XK1
901 X(K,2)=XK2
  XMAX(1,1)=XMAX1
  XMAX(1,2)=XMAX2
  XMAX1=0.0
  XMAX2=0.0
  DO 902 K=1,NV
    XX=X(K,1)
    XY=X(K,2)
    XK1=XX*XX1+XY*XY2
    XK2=XY*XX1-XX*XY2
    XMAX1=AMAX1(XMAX1,ABS(XK1))
    XMAX2=AMAX1(XMAX2,ABS(XK2))
    XD(K,1)=XK1
902 XD(K,2)=XK2
  XMAX(2,1)=XMAX1
  XMAX(2,2)=XMAX2
  IF(IND1.EQ.0) GO TO 10
  CALL PRINP(TETA,NA,NV)
10 IF(IND2.EQ.0) GO TO 20
  CALL PUINP(NA,NV)
20 IF(IND3.EQ.0) GO TO 30
30 CONTINUE
  STOP
40 FORMAT(8A10)
100 FORMAT(2F10.0)
101 FORMAT(3I1)
  END

```

```

SUBROUTINE INPUT(NA)
DIMENSION CORTIL(250),ICOR(100),FCOR(100),IX(5000,2),
          XDD(1250,2)
COMMON /DATAN/X(2501,2),XD(2500,2),XMAX(2,2)
DO 900 I=1,2
110 READ(1,50) CORTIL
  IF(EOF,1) 110,9
9 READ(1,60) ICOR
  NDATA=ICOR(53)
  NDATV=ICOR(64)
  NDATD=ICOR(66)
  READ(1,70) FCOR
  READ(1,60) (IX(K,II),K=1,NDATA)
  READ(1,80) (XD(K,II),K=1,NDATV)
  READ(1,80) (XDD(K,II),K=1,NDATD)
  DO 800 K=1,NA
    X(K,II)=FLOAT(IX(K,II))*0.1
800 CONTINUE
900 CONTINUE
  RETURN
50 FORMAT(10A10)
60 FORMAT(10I10)
70 FORMAT(10F10.5)
80 FORMAT(10F10.3)
  END

```

```

SUBROUTINE PRINP(TETA,NA,NV)
COMMON /DATAN/X(2501,2),XD(2500,2),XMAX(2,2)
COMMON /N11/NAME(8)
DO 909 I=1,2
  WRITE(6,51) NAME
  GO TO(1,2),I
1 WRITE(6,52)
  GO TO 3
2 WRITE(6,53)
3 WRITE(6,54) XMAX(1,II),TETA,NA
  WRITE(6,55) (X(K,II),K=1,NA)
  WRITE(6,51) NAME
  GO TO(4,5),I
4 WRITE(6,52)
  GO TO 6
5 WRITE(6,53)
6 WRITE(6,56) XMAX(2,II),TETA,NV
  WRITE(6,57) (XD(K,II),K=1,NV)
909 CONTINUE
  RETURN
51 FORMAT(1H1,2X,8A10)
52 FORMAT(1H ,2X,22HLONGITUDINAL COMPONENT)
53 FORMAT(1H ,2X,20HTRANSVERSE COMPONENT)
54 FORMAT(1H0,80X,9HACC. MAX=F10.4/1H ,80X,5HTETA=F14.4/
  1 1H ,80X,3HNA=.116/1H ,80X,14HDT= 9.02 (SEC)/
  2 1H ,80X,14HFMT= (10F10.1)/)
55 FORMAT(1H ,10F10.1)
56 FORMAT(1H0,80X,9HVEL. MAX=F10.4/1H ,80X,5HTETA=F14.4/
  1 1H ,80X,3HNV=.116/1H ,80X,14HDT= 8.04 (SEC)/
  2 1H ,80X,14HFMT= (10F10.3)/)
57 FORMAT(1H ,10F10.3)
  END

```

```

SUBROUTINE PUINP(NA,NV)
COMMON /DATAN/X(2501,2),XD(2500,2),XMAX(2,2)
COMMON /N11/NAME(8)
DO 910 I=1,2
  PUNCH 71,NAME
  GO TO(1,2),I
1 PUNCH 72
  GO TO 3
2 PUNCH 73
3 PUNCH 74,XMAX(1,II)
  PUNCH 77,NA
  PUNCH 75,(X(K,II),K=1,NA)
  PUNCH 71,NAME
  GO TO(4,5),I
4 PUNCH 72
  GO TO 6
5 PUNCH 73
6 PUNCH 74,XMAX(2,II)
  PUNCH 78,NV
  PUNCH 76,(XD(K,II),K=1,NV)
910 CONTINUE
  RETURN
71 FORMAT(8A10)
72 FORMAT(18HLONGITUDINAL COMP.)
73 FORMAT(16HTRANSVERSE COMP.)
74 FORMAT(F10.4)
75 FORMAT(10F7.1)
76 FORMAT(10F7.3)
77 FORMAT(15/4H0.02/8H(10F7.1))
78 FORMAT(15/4H0.04/8H(10F7.3))
  END

```

```

EL CENTRO 1940.5.18 IMPERIAL VALLEY
50.0
54.5
111

```

```

PROGRAM RUNF1(INPUT,OUTPUT,TAPES=INPUT,TAPES=OUTPUT,PUNCH)
INPUT DATA
  NG - NUMBER OF DIVIDED INTERVALS
  NAMI - NAME OF EACH INTERVAL
  N11,NN1 - STEP NUMBER OF START AND END OF EACH INTERVAL
  NAME - NAME OF STATION AND EARTHQUAKE
  NE - TOTAL NUMBER OF EARTHQUAKE DATA
  DT - TIME INTERVAL OF DATA (SEC)
  FMT - FORMAT OF DATA
  XD - EARTHQUAKE DATA
PUNCHED CARDS BY PROGRAM (CORIN) CAN BE USED AS NAME TO XD DIRECTLY.
DIMENSION NAME(8),NAMI(2),NAMI(2,5),N11(5),N11(5)
DIMENSION X(2501),XD(1251),XX(2501),XXX(2501)
COMPLEX C(4096)
READ(5,12) NG
12 FORMAT(2I5)
DO 21 I=1,NG
  READ(5,10) (NAMI(J,I),J=1,2)
  READ(5,12) N11(I),NN1(I)
21 CONTINUE
READ(5,10) NAME
10 FORMAT(8A10)
READ(5,11) NE,DT,FMT
11 FORMAT(//15/F10.0/A10)
READ(5,FMT) (XD(K),K=1,NE)
DO 1000 I=1,NG
  N1=N11(I)
  NN=NN1(I)-N1+1
  DO 22 J=1,2
22 NAMI(J)=NAMI(J,I)
  WRITE(6,81) NAME
81 FORMAT(1H1,2X,8A10)
  WRITE(6,92) NAMI,N1,NN,DT
92 FORMAT(1H ,70X,2A10/1H0,20X,3NN1=,15/1H ,20X,3NN=,15/1H ,80X,3HDT=,F5.2,6H (SEC)/)
  N=512
  IF(NN.GT.N) N=1024
  IF(NN.GT.N) N=2048
  IF(NN.GT.N) N=4096
  IF(NN.LE.N) GO TO 201
  DO 200 K=1,N
    J=N1+K-1
200 C(K)=CMPLX(XD(J),0.0)
    GO TO 204
201 DO 202 K=1,NN
    J=N1+K-1
202 C(K)=CMPLX(XD(J),0.0)
    NE=NN+1
    DO 203 K=NE,N
203 C(K)=CMPLX(0.0,0.0)
204 CALL FAST(N,C,4096,-1)
    AN=FLOAT(N)
    DO 209 K=1,N
209 C(K)=C(K)/AN
    N2=N/2
    DO 205 K=1,N2
    AC=C(K)
    PC=C(K)*(0.0,-1.0)
    XX(K)=CABS(C(K))*2.0
205 XXX(K)=ATAN(PC/AC)
    WRITE(6,80) C(1),XX(1),XXX(1)
80 FORMAT(7X,1H0,3X,5HF(AZ),2X,6HT(SEC),11X,4HC(K),8X,11HAMP(CM/SEC),1X,9HPHA1(RAD)/1H ,6X,21H1,3X,3H0,0,5X,3H---,4X,2F10.4,2X,2F10.4,E15.6,F11.5)
    DF=1./DT*AN
    F=0.0
    DO 206 K=2,N2
    F=F+DF
    TF=1./F
    WRITE(6,91) K,F,TF,C(K),XX(K),XXX(K)
91 FORMAT(1H ,17,2F8.3,2X,2F10.4,2X,2F10.4)
206 CONTINUE
PUNCH 300,NAME
300 FORMAT(8A10)
PUNCH 302,NAM
302 FORMAT(2A10)
PUNCH 301,(XX(K),K=1,N2)
301 FORMAT(10F7.4)
PUNCH 301,(XXX(K),K=1,N2)
CALL SPAR(NAME,N2,XX,2501,DF,100.0,NAM)
1000 CONTINUE
STOP
END

```

```

*****
SUBROUTINE FOR FAST FOURIER TRANSFORM
*****
SUBROUTINE FAST(N,X,ND,IND)

```

CODED BY Y. OHSAKI

PURPOSE

TO PERFORM FAST FOURIER OR INVERSE FOURIER TRANSFORM FOR A SERIES OF EQUI-SPACED DATA

USAGE

CALL FAST(N,X,ND,IND)

DESCRIPTION OF PARAMETERS

N - TOTAL NUMBER OF COMPLEX DATA AND TRANSFORMED VALUES
 X(ND) - EQUI-SPACED COMPLEX DATA/TRANSFORMED VALUES AT CALL/RETURN
 ND - DIMENSION OF X IN CALLING PROGRAM
 IND - IND=-1 FOR FOURIER TRANSFORM
 +1 FOR INVERSE FOURIER TRANSFORM

REMARKS

(1) N MUST BE EQUAL TO POWERS OF 2
 (2) WHEN IND=-1, TRANSFORMED VALUES ARE MULTIPLIED BY N
 (3) EXAMPLE OF CALLING

```

COMPLEX A(1024)
DIMENSION DATA(1024)
DATA NN/1024/
DO 1 M=1,NN
  A(M)=CMPLX(DATA(M),0.0)
1 CONTINUE
CALL FAST(NN,A,1024,-1)

```

REFERENCE

N.M.BRENNER / THREE FORTRAN PROGRAMS THAT PERFORM THE COOLEY-TUKEY FOURIER TRANSFORM / MIT JULY 1967

SUBROUTINES AND FUNCTION SUBPROGRAMS REQUIRED
 NONE

COMPLEX X(ND),TEMP,THETA

```

J=1
DO 140 I=1,N
  IF(1.GE.J) GO TO 110
  TEMP=X(J)
  X(J)=X(I)
  X(I)=TEMP
110 M=N/2
120 IF(J.LE.M) GO TO 130
  J=J-M
  M=M/2
130 J=J+M
140 CONTINUE
  KMAX=1
150 IF(KMAX.GE.N) RETURN
  ISTEP=KMAX*2
  DO 170 K=1,KMAX
  THETA=CMPLX(0.0,3.141593*FLOAT(IND*(K-1))/FLOAT(KMAX))
  DO 160 I=K,N,ISTEP
    J=I+KMAX
    TEMP=X(J)*CEXP(THETA)
    X(J)=X(I)-TEMP
    X(I)=X(I)+TEMP
160 CONTINUE
170 CONTINUE
  KMAX=ISTEP
  GO TO 150
END

```

```

C
C *****
C SUBROUTINE FOR PRINT OF SPECTRA AND AUTOCORRELATION
C *****
C SUBROUTINE SPAR(NAME,N,Y,ND,DX,IND,IAXIS,NAM)
C
C CODED BY Y. OHSAKI
C
C PURPOSE
C TO PRINT ON LINE-PRINTER APPROXIMATE SHAPE OF FOURIER, POWER
C SPECTRA OR AUTOCORRELATION
C
C USAGE
C CALL SPAR(NAME,N,Y,ND,DX,IND,IAXIS)
C
C DESCRIPTION OF PARAMETERS
C NAME( 8) - NAME OF DATA
C N       - TOTAL NUMBER OF SPECTRAL VALUES OR AUTOCORRELATION
C          COEFFICIENTS
C Y(ND)  - SPECTRAL VALUES OR AUTOCORRELATION COEFFICIENTS
C ND     - DIMENSION OF Y IN CALLING PROGRAM
C DX     - FREQUENCY INCREMENT IN CYCLES/SEC IN FOURIER OR
C          POWER SPECTRUM, OR LAG INCREMENT IN SEC IN AUTOCOR-
C          RELATION
C
C IND    - 100 FOR PRINT OF FOURIER SPECTRUM
C          010 FOR PRINT OF POWER SPECTRUM
C          001 FOR PRINT OF AUTOCORRELATION
C
C IAXIS  - IF 0, VERTICAL SCALE IS NEWLY DEFINED
C          IF 1, VERTICAL SCALE IN PREVIOUS CALL IS RETAINED
C
C REMARKS
C (1) AUTOCORRELATION MUST HAVE BEEN NORMALIZED IN TERMS OF MEAN
C     SQUARED VALUE OF DATA
C (2) FOR IND=001(AUTOCORRELATION), IAXIS HAS NO MEANING
C
C SUBROUTINES AND FUNCTION SUBPROGRAMS REQUIRED
C NONE
C
C DIMENSION NAME( 8),Y(ND)
C DIMENSION NAM(2)
C DIMENSION L(101),SMAJ(4),STEP(4),LSTEP(4),FMT(3),FMT3(6),NUM(9)
C DATA SMAJ/2.,4.,5.,10./,STEP/5,1,1,2./,LSTEP/10,10,8,8/
C DATA FMT3/4H.1),4H.2),4H.3),4H.4),4H.5),4H.6) /
C DATA NUM/1H1,1H2,1H3,1H4,1H5,1H6,1H7,1H8,1H9/
C
C HEADING
C
C WRITE(6,601) NAME
C WRITE(6,701) NAM
C IF(IND.EQ.100) WRITE(6,602)
C IF(IND.EQ.010) WRITE(6,603)
C IF(IND.EQ.001) WRITE(6,604)
C IF(IND.EQ.001) GO TO 140
C YMAX=0.0
C DO 110 K=1,N
C YMAX=AMAX1(YMAX,Y(K))
110 CONTINUE
C WRITE(6,605) YMAX
C
C VERTICAL SCALE
C
C IF(IAXIS.EQ.1) GO TO 160
C M=FIX(ALOG10(YMAX))
C IF(ALOG10(YMAX).LT.0.0) M=M-1
C DO 120 J=1,4
C IF(YMAX/10.0**M.LE.SMAJ(J)) GO TO 130
120 CONTINUE
C SMAJ=SMAJ(J)*10.0**M
C STEP=STEP(J)*10.0**M
C LSTEP=LSTEP(J)
C IF(4.GT.0) FMT(3)=4H.0)
C IF(4.LE.0) FMT(3)=FMT3(1-M)
C LINE0=41
C XMAX=10.0
C GO TO 150
140 SMAJ=1.0
C STEP=0.5
C LSTEP=10
C FMT(3)=4H.1)
C LINE0=21
C XMAX=5.0
150 FMT(1)=4H(1H+
C FMT(2)=4H.F13
C
C PRINT
160 NSTEP=MAX1(XMAX/DX/100.0+0.0001,1.0)
C IF(IND.EQ.001) GO TO 180
C IF(IAXIS.EQ.0) COR=40.0/SMAJ
C DO 170 K=1,N,NSTEP
C Y(K)=Y(K)*COR
170 CONTINUE
C GO TO 200
180 DO 190 K=1,N,NSTEP
C Y(K)=(Y(K)+1.0)*20.0
190 CONTINUE
200 SCALE=SMAJ
C DO 250 LINE=1,41
C L(1)=1H1
C LI=1H
C IF(LINE.EQ.LINE0) LI=1H-
C DO 210 I=2,101
C L(I)=LI
210 CONTINUE
C BU=FLOAT(41-LINE)+0.5
C BL=FLOAT(41-LINE)-0.5
C DO 220 K=1,N,NSTEP
C IF(FLOAT(K-1)*DX.GT.XMAX) GO TO 230
C IF(Y(K).GE.BU.OR.Y(K).LT.BL) GO TO 220
C LL=FIX(FLOAT(K-1)*DX/XMAX*100.0+0.5)+1
C L(LL)=1H*
220 CONTINUE
C WRITE(6,606)
C IF(MOD(LINE,LSTEP),NE.1) GO TO 240
C WRITE(6,FMT) SCALE
C SCALE=SCALE*STEP
240 WRITE(6,607) L
250 CONTINUE
C
C HORIZONTAL SCALE
C
C L(1)=1H0
C DO 260 I=2,101
C L(I)=1H
260 CONTINUE
C DO 270 I=1,9
C INUM=FIX(100.0/XMAX)*I+1
C IF(INUM.GT.101) GO TO 280
C L(INUM)=NUM(I)
270 CONTINUE
280 WRITE(6,608) L
C IF(IND.NE.001) WRITE(6,609)
C IF(IND.EQ.001) WRITE(6,610)
C RETURN
C
C FORMAT STATEMENTS
C
C 601 FORMAT(1H1,10X,8A10)
C 602 FORMAT(1H0,12X,22H-- FOURIER SPECTRUM --)
C 603 FORMAT(1H0,12X,20H-- POWER SPECTRUM --)
C 604 FORMAT(1H0,12X,21H-- AUTOCORRELATION --/1H0/)
C 605 FORMAT(1H0,90X,4HMAX.,F13.5/)
C 606 FORMAT(1H)
C 607 FORMAT(1H+,14X,10I1)
C
C 608 FORMAT(1H0,14X,10I1/)
C 609 FORMAT(1H0,57X,15HFREQUENCY (CPS))
C 610 FORMAT(1H0,50X,13HTIME LAG(SEC))
C 701 FORMAT(1H+,08X,2A10)
C
C END

```

```

PROGRAM CORFA(INPUT,OUTPUT,TAPE5=INPUT,TAPE6=OUTPUT,TAPE9)
INPUT DATA
DT      - TIME INTERVAL OF EARTHQUAKE DATA
FMAX    - MAXIMUM FREQUENCY ON FIGURE OF FOURIER SPECTRUM
NG      - NUMBER OF DIVIDED INTERVALS
NF      - NUMBER OF NP
NP      - 1-2 FOR NS-EW, LO-TR OR CO-SH
          2-3 FOR EW-COR, NS, TR-COR, LO OR SH-COR, CO
          1-4 FOR NS-COR, EW, LO-COR, TR OR CO-COR, SH
N       - NUMBER OF COMPLEX FOURIER FREQUENCIES
YMAX, DIVY- MAX. VALUE AND NUMBER OF EQUAL DIVISIONS ON ORDINATE
NAME    - NAME OF STATION AND EARTHQUAKE
NAM     - NAME OF EACH DIVIDED INTERVAL
AMP     - FOURIER AMPLITUDE
PHAI    - PHASE DIFFERENCE
FMAX CAN BE SELECTED ARBITRARILY.
PUNCHED CARDS BY PROGRAM (RUNFI) CAN BE USED AS NAME TO PHAI
DIRECTLY.
AMP(K,1) = ORIGINAL FOURIER AMPLITUDE NS OR LO
AMP(K,2) = ORIGINAL FOURIER AMPLITUDE EW OR TR
AMP(K,3) = CORRECTED FOURIER AMPLITUDE NS OR LO
AMP(K,4) = CORRECTED FOURIER AMPLITUDE EW OR TR
DIMENSION NAME( 3,2),NAM(2,2),AMP(2048,4),PHAI(2048,4)
DIMENSION NAM1( 8),NAM2(2)
DIMENSION X(2048),Y(2048),DIVY(5),YMAX(5),NP(2,3)
DIMENSION SPECS(35)
READ(5,102) DT
READ(5,102) FMAX
READ(5,100) NG
READ(5,100) NF
DO 1 J=1,NF
1 READ(5,100) (NP(J,1),J=1,2)
100 FORMAT(8I5)
XFRM=1.5
DO 999 I=1,NG
READ(5,100) N
READ(5,102) YMAX(I),DIVY(I)
N2=N/2
AN=FLOAT(N)
DO 10 I=1,2
READ(5,101) (NAME(J,I),J=1,8)
101 FORMAT(8A10)
READ(5,103) (NAM(J,I),J=1,2)
103 FORMAT(2A10)
102 FORMAT(10F7.0)
READ(5,102) (AMP(K,1),K=1,N2)
READ(5,102) (PHAI(K,1),K=1,N2)
10 CONTINUE
DO 20 K=1,N2
AMP1=AMP(K,1)
AMP2=AMP(K,2)
PHAI1=PHAI(K,1)
PHAI2=PHAI(K,2)
P1=PHAI1-PHAI2
P2=PHAI2-PHAI1
AMP3=AMP1*COS(P1)
AMP4=AMP2*COS(P2)
PHAI(K,3)=AMP3/AMP1
PHAI(K,4)=AMP4/AMP2
AMP(K,3)=AMP3
AMP(K,4)=AMP4
20 CONTINUE
XFRM=XFRM+44.0*FLOAT(I-1)
DO 990 JJ=1,NF
SPECS( 1)=XFRM
SPECS( 2)=3.0
SPECS( 7)=10.0
SPECS( 8)=5.0
SPECS( 9)=10.0
SPECS(10)= DIVY(I)
SPECS(11)=1.
SPECS(12)=99.
CALL AXLILI(SPECS)
SPECS( 3)=FMAX
SPECS( 4)=0.0
SPECS(17)=0.12
SPECS(18)=0.18
SPECS(19)=0.0
SPECS(21)=1.0
SPECS(24)=0.0
SPECS(28)=1.0
CALL MODLIB(SPECS)
SPECS( 5)=YMAX(I)
SPECS( 6)=0.0
SPECS(20)=0.0
SPECS(26)=0.0
CALL MODLIL(SPECS)
CALL TITLEB(14HFREQUENCY (HZ),SPECS)
CALL TITLEL(17HFOURIER AMPLITUDE,SPECS)
DF=1./(DT*N)
F=0.0
DO 30 K=1,N2
X(K)=F
F=F+DF
IF(F.GT.FMAX) GO TO 31
30 CONTINUE
31 NEND=K-1
SPECS(13)=FLOAT(NEND)
YMAX=0.0
DO 50 J=1,2
NPJ=NP(J,1)
DO 40 K=1,NEND
YK=ABS(AMP(K,NPJ))
YMAX=AMAX1(YMAX,YK)
40 Y(K)=YK
IF(J.EQ.2) SPECS(11)=2.
SPECS(14)=1.0
SPECS(15)=1.0
CALL SLLILI(X,Y,SPECS)
50 CONTINUE
SPECS(11)=1.
SPECS(22)= XFRM+0.1
SPECS(23)= 8.5
DO 51 J=1,7
51 NAM1(J)=NAME(J,1)
RULE=1.
NAM1(8)=0
CALL TITLEG(RULE,NAM1,SPECS)
SPECS(22)=XFRM+7.5
SPECS(23)=8.0
NP2=NP(2,1)
IF(NP2.GT.2) GO TO 41
CALL TITLEG(RULE,9HOR1.-OR1.,SPECS)
GO TO 42
41 CALL TITLEG(RULE,9HOR1.-COR.,SPECS)
42 CONTINUE
DO 54 I=1,2
INF=1.
JNF=2-I+1
IF(MOD(NP(1,1),2)
IF(JF.EQ.0) INF=JNF
DO 52 J=1,2
52 NAM2(J)=NAM(J,INF)
SPECS(23)=7.8
IF(I.EQ.2) GO TO 53
SPECS(23)=7.6
SPECS(11)=2.
53 CALL TITLEG(RULE,NAM2,SPECS)
54 CONTINUE
SPECS(11)=1.
SPECS(23)=7.4
CALL TITLEG(RULE,4HMAX=.SPECS)
SPECS(22)=XFRM+8.2
SPECS(28)=3.0
CALL DECVAL(RULE,YMAX,SPECS)
XFRM=XFRM+14.0
990 CONTINUE
999 CONTINUE
CALL GDSND(SPECS)
STOP
END

```

```

PROGRAM PLWAVE(INPUT,OUTPUT,TAPE5=INPUT,TAPE6=OUTPUT,TAPE99)
INPUT DATA
ILN      - #1 CASE OF COORDINATE TRANSFORMATION TO
          LONGITUDINAL AND TRANSVERSE DIRECTION TOWARD
          EPICENTER
          #2 CASE OF COORDINATE TRANSFORMATION TO
          NORMAL AND PARALLEL DIRECTION TO FAULT LINE
NAME     - NAME OF STATION AND EARTHQUAKE
XMAX(1,II)- MAXIMUM VALUE OF ACCELERATION (GAL)
NA      - TOTAL NUMBER OF X
X       - ACCELERATION DATA
XMAX(2,II)- MAXIMUM VALUE OF VELOCITY (KINE)
NV      - TOTAL NUMBER OF XD
XD      - VELOCITY DATA
PUNCHED CARDS BY PROGRAM (CORIN) CAN BE USED AS NAME TO XD
DIRECTLY.
II=1-LONGITUDINAL DATA, #2-TRANSVERSE DATA
III=1-ACC. DATA, #2-VEL. DATA
DIMENSION XMAL(2),XSC(7)
COMMON /DATAN/X(3000,2),XD(1500,2),XMAX(2,2)
COMMON /N11/NAME(8)
COMMON /ILOND/ILN
DATA XSC/10.,20.,30.,40.,50.,60.,100./
READ(5,1) ILN
DO 10 II=1,2
READ(5,100) NAME,XMAX(1,II),NA
READ(5,101) (X(K,II),K=1,NA)
READ(5,102) XMAX(2,II),NV
READ(5,101) (XD(K,II),K=1,NV)
10 CONTINUE
XM=0.0
DO 50 III=1,2
DO 20 II=1,2
XM=AMAX1(XM,XMAX(III,II))
20 CONTINUE
IF(III.EQ.1) XM=XM*0.1
XPM=100.
IF(XM.GE.XPM) GO TO 40
XPM=XM
IF(XM.LE.XPM) GO TO 40
DO 30 KK=1,7
IF(XM.GT.XSC(KK)) GO TO 30
XPM=XSC(KK)
GO TO 40
30 CONTINUE
40 IF(III.EQ.1) XPM=XPM*10.
XMAL(III)=XPM
50 CONTINUE
CALL PLINP(NA,NV,XMAL)
STOP
1 FORMAT(15)
100 FORMAT(8A10//F10.4/15//)
101 FORMAT(10F7.0)
102 FORMAT(//F10.4/15//)
END

SUBROUTINE PLINP(NA,NV,XMAL)
III=1-PLOT OF ACC. DATA, #2-PLOT OF VEL. DATA
II=1-PLOT OF LONGITUDINAL DATA, #2-PLOT OF TRANSVERSE DATA
DIMENSION T1(2501),Y(2501),S(35),GXS(4),XTI(3,2),YTI(3,2)
DIMENSION XMAL(2)
COMMON /DATAN/X(3000,2),XD(1500,2),XMAX(2,2)
COMMON /N11/NAME(8)
COMMON /ILOND/ILN
XFRM=1.5
DO 500 III=1,2
T1(1)=0.0
T11=0.02
NAV=NA
IF(III.EQ.1) GO TO 349
T11=0.04
NAV=NV
349 DO 350 K=2,NAV
350 T1(K)=T11*FLOAT(K-1)
DO 400 II=1,2
YFRM=3.*FLOAT(II-1)
S(1)=XFRM
S(2)=3.0+YFRM
S(3)=T1(NAV)
S(4)=0.
S(5)=XMAL(III)
S(6)=-S(5)
S(7)=20.
S(8)=2.
S(11)=1.
S(12)=99.
GXS(1)=0.
GXS(2)=0.
GXS(3)=1.
GXS(4)=1.
XTI(1,1)=3.0
XTI(2,1)=0.3
XTI(3,1)=10.0
YTI(1,1)=1.0
YTI(2,1)=0.15
YTI(3,1)=2.0
CALL GXLILI(GXS,XTI,YTI,S)
S(9)=5.
S(17)=0.12
S(18)=0.18
S(19)=0.0
S(20)=0.0
S(21)=1.
S(24)=0.0
S(28)=1.
CALL MODLIB(S)
RULE=1.
S(22)=XFRM+19.6
S(23)=2.5+YFRM
CALL TITLEG(RULE,5H(SEC),S)
S(10)=2.
S(26)=0.0
CALL MODLIB(S)
DO 380 K=1,NAV
GO TO(378,379),III
378 Y(K)=X(K,II)
GO TO 380
379 Y(K)=XD(K,II)
380 CONTINUE
S(13)=NAV
S(14)=1.
S(15)=1.
CALL SLLILI(T1,Y,S)
S(22)=XFRM+16.5
S(23)=YFRM+4.7
GO TO(392,492),ILN
392 GO TO(393,396),II
393 GO TO(394,395),III
394 CALL TITLEG(RULE,22HLONGITUDINAL ACC.(GAL),S)
GO TO 399
395 CALL TITLEG(RULE,23HLONGITUDINAL VEL.(KINE),S)
GO TO 399
396 GO TO(397,398),III
397 CALL TITLEG(RULE,20HTRANSVERSE ACC.(GAL),S)
GO TO 399
398 CALL TITLEG(RULE,21HTRANSVERSE VEL.(KINE),S)
GO TO 399
492 GO TO(493,496),II
493 GO TO(494,495),III
494 CALL TITLEG(RULE,25HNORMAL TO FAULT ACC.(GAL),S)
GO TO 399
495 CALL TITLEG(RULE,26HNORMAL TO FAULT VEL.(KINE),S)
GO TO 399
496 GO TO(497,498),III
497 CALL TITLEG(RULE,27HPARALLEL TO FAULT ACC.(GAL),S)
GO TO 399
498 CALL TITLEG(RULE,26HPARALLEL TO FAULT VEL.(KINE),S)
399 S(23)=S(23)-0.25
CALL TITLEG(RULE,4HMAX*,S)
S(22)=S(22)+0.9
IF(III.EQ.2) S(28)=3.
CALL DECVL(RULE,XMAX(III,II),S)
400 CONTINUE
S(22)=S(1)+0.2
S(23)=0.4
NAME(8)=0
CALL TITLEG(RULE,NAME,S)
XFRM=XFRM+25.0
500 CONTINUE
CALL GDSEND(S)
RETURN
END

```


EARTHQUAKE ENGINEERING RESEARCH CENTER REPORTS

NOTE: Numbers in parenthesis are Accession Numbers assigned by the National Technical Information Service; these are followed by a price code. Copies of the reports may be ordered from the National Technical Information Service, 5285 Port Royal Road, Springfield, Virginia, 22161. Accession Numbers should be quoted on orders for reports (PB --- ---) and remittance must accompany each order. Reports without this information were not available at time of printing. Upon request, EERC will mail inquirers this information when it becomes available.

- EERC 67-1 "Feasibility Study Large-Scale Earthquake Simulator Facility," by J. Penzien, J.G. Bouwkamp, R.W. Clough and D. Rea - 1967 (PB 187 905)A07
- EERC 68-1 Unassigned
- EERC 68-2 "Inelastic Behavior of Beam-to-Column Subassemblages Under Repeated Loading," by V.V. Bertero - 1968 (PB 184 888)A05
- EERC 68-3 "A Graphical Method for Solving the Wave Reflection-Refraction Problem," by H.D. McNiven and Y. Mengi - 1968 (PB 187 943)A03
- EERC 68-4 "Dynamic Properties of McKinley School Buildings," by D. Rea, J.G. Bouwkamp and R.W. Clough - 1968 (PB 187 902)A07
- EERC 68-5 "Characteristics of Rock Motions During Earthquakes," by H.B. Seed, I.M. Idriss and F.W. Kiefer - 1968 (PB 188 338)A03
- EERC 69-1 "Earthquake Engineering Research at Berkeley," - 1969 (PB 187 906)A11
- EERC 69-2 "Nonlinear Seismic Response of Earth Structures," by M. Dibaj and J. Penzien - 1969 (PB 187 904)A08
- EERC 69-3 "Probabilistic Study of the Behavior of Structures During Earthquakes," by R. Ruiz and J. Penzien - 1969 (PB 187 886)A06
- EERC 69-4 "Numerical Solution of Boundary Value Problems in Structural Mechanics by Reduction to an Initial Value Formulation," by N. Distefano and J. Schujman - 1969 (PB 187 942)A02
- EERC 69-5 "Dynamic Programming and the Solution of the Biharmonic Equation," by N. Distefano - 1969 (PB 187 941)A03
- EERC 69-6 "Stochastic Analysis of Offshore Tower Structures," by A.K. Malhotra and J. Penzien - 1969 (PB 187 903)A09
- EERC 69-7 "Rock Motion Accelerograms for High Magnitude Earthquakes," by H.B. Seed and I.M. Idriss - 1969 (PB 187 940)A02
- EERC 69-8 "Structural Dynamics Testing Facilities at the University of California, Berkeley," by R.M. Stephen, J.G. Bouwkamp, R.W. Clough and J. Penzien - 1969 (PB 189 111)A04
- EERC 69-9 "Seismic Response of Soil Deposits Underlain by Sloping Rock Boundaries," by H. Dezfulian and H.B. Seed - 1969 (PB 189 114)A03
- EERC 69-10 "Dynamic Stress Analysis of Axisymmetric Structures Under Arbitrary Loading," by S. Ghosh and E.L. Wilson - 1969 (PB 189 026)A10
- EERC 69-11 "Seismic Behavior of Multistory Frames Designed by Different Philosophies," by J.C. Anderson and V. V. Bertero - 1969 (PB 190 662)A10
- EERC 69-12 "Stiffness Degradation of Reinforcing Concrete Members Subjected to Cyclic Flexural Moments," by V.V. Bertero, B. Bresler and H. Ming Liao - 1969 (PB 202 942)A07
- EERC 69-13 "Response of Non-Uniform Soil Deposits to Travelling Seismic Waves," by H. Dezfulian and H.B. Seed - 1969 (PB 191 023)A03
- EERC 69-14 "Damping Capacity of a Model Steel Structure," by D. Rea, R.W. Clough and J.G. Bouwkamp - 1969 (PB 190 663)A06
- EERC 69-15 "Influence of Local Soil Conditions on Building Damage Potential during Earthquakes," by H.B. Seed and I.M. Idriss - 1969 (PB 191 036)A03
- EERC 69-16 "The Behavior of Sands Under Seismic Loading Conditions," by M.L. Silver and H.B. Seed - 1969 (AD 714 982)A07
- EERC 70-1 "Earthquake Response of Gravity Dams," by A.K. Chopra - 1970 (AD 709 640)A03
- EERC 70-2 "Relationships between Soil Conditions and Building Damage in the Caracas Earthquake of July 29, 1967." by H.B. Seed, I.M. Idriss and H. Dezfulian - 1970 (PB 195 762)A05
- EERC 70-3 "Cyclic Loading of Full Size Steel Connections," by E.P. Popov and R.M. Stephen - 1970 (PB 213 545)A04
- EERC 70-4 "Seismic Analysis of the Charaima Building, Caraballeda, Venezuela," by Subcommittee of the SEAONC Research Committee: V.V. Bertero, P.F. Fratessa, S.A. Mahin, J.H. Sexton, A.C. Scordelis, E.L. Wilson, L.A. Wyllie, H.B. Seed and J. Penzien, Chairman - 1970 (PB 201 455)A06

- EERC 70-5 "A Computer Program for Earthquake Analysis of Dams," by A.K. Chopra and P. Chakrabarti - 1970 (AD 723 994)A05
- EERC 70-6 "The Propagation of Love Waves Across Non-Horizontally Layered Structures," by J. Lysmer and L.A. Drake 1970 (PB 197 896)A03
- EERC 70-7 "Influence of Base Rock Characteristics on Ground Response," by J. Lysmer, H.B. Seed and P.B. Schnabel 1970 (PB 197 897)A03
- EERC 70-8 "Applicability of Laboratory Test Procedures for Measuring Soil Liquefaction Characteristics under Cyclic Loading," by H.B. Seed and W.H. Peacock - 1970 (PB 198 016)A03
- EERC 70-9 "A Simplified Procedure for Evaluating Soil Liquefaction Potential," by H.B. Seed and I.M. Idriss - 1970 (PB 198 009)A03
- EERC 70-10 "Soil Moduli and Damping Factors for Dynamic Response Analysis," by H.B. Seed and I.M. Idriss - 1970 (PB 197 869)A03
- EERC 71-1 "Koyna Earthquake of December 11, 1967 and the Performance of Koyna Dam," by A.K. Chopra and P. Chakrabarti 1971 (AD 731 496)A06
- EERC 71-2 "Preliminary In-Situ Measurements of Anelastic Absorption in Soils Using a Prototype Earthquake Simulator," by R.D. Borcherdt and P.W. Rodgers - 1971 (PB 201 454)A03
- EERC 71-3 "Static and Dynamic Analysis of Inelastic Frame Structures," by F.L. Porter and G.H. Powell - 1971 (PB 210 135)A06
- EERC 71-4 "Research Needs in Limit Design of Reinforced Concrete Structures," by V.V. Bertero - 1971 (PB 202 943)A04
- EERC 71-5 "Dynamic Behavior of a High-Rise Diagonally Braced Steel Building," by D. Rea, A.A. Shah and J.G. Bonwhamp 1971 (PB 203 584)A06
- EERC 71-6 "Dynamic Stress Analysis of Porous Elastic Solids Saturated with Compressible Fluids," by J. Ghaboussi and E. L. Wilson - 1971 (PB 211 396)A06
- EERC 71-7 "Inelastic Behavior of Steel Beam-to-Column Subassemblages," by H. Krawinkler, V.V. Bertero and E.P. Popov 1971 (PB 211 335)A14
- EERC 71-8 "Modification of Seismograph Records for Effects of Local Soil Conditions," by P. Schnabel, H.B. Seed and J. Lysmer - 1971 (PB 214 450)A03
- EERC 72-1 "Static and Earthquake Analysis of Three Dimensional Frame and Shear Wall Buildings," by E.L. Wilson and H.H. Dovey - 1972 (PB 212 904)A05
- EERC 72-2 "Accelerations in Rock for Earthquakes in the Western United States," by P.B. Schnabel and H.B. Seed - 1972 (PB 213 100)A03
- EERC 72-3 "Elastic-Plastic Earthquake Response of Soil-Building Systems," by T. Minami - 1972 (PB 214 868)A08
- EERC 72-4 "Stochastic Inelastic Response of Offshore Towers to Strong Motion Earthquakes," by M.K. Kaul - 1972 (PB 215 713)A05
- EERC 72-5 "Cyclic Behavior of Three Reinforced Concrete Flexural Members with High Shear," by E.P. Popov, V.V. Bertero and H. Krawinkler - 1972 (PB 214 555)A05
- EERC 72-6 "Earthquake Response of Gravity Dams Including Reservoir Interaction Effects," by P. Chakrabarti and A.K. Chopra - 1972 (AD 762 330)A08
- EERC 72-7 "Dynamic Properties of Pine Flat Dam," by D. Rea, C.Y. Liaw and A.K. Chopra - 1972 (AD 763 928)A05
- EERC 72-8 "Three Dimensional Analysis of Building Systems," by E.L. Wilson and H.H. Dovey - 1972 (PB 222 438)A06
- EERC 72-9 "Rate of Loading Effects on Uncracked and Repaired Reinforced Concrete Members," by S. Mahin, V.V. Bertero, D. Rea and M. Atalay - 1972 (PB 224 520)A08
- EERC 72-10 "Computer Program for Static and Dynamic Analysis of Linear Structural Systems," by E.L. Wilson, K.-J. Bathe, J.E. Peterson and H.H. Dovey - 1972 (PB 220 437)A04
- EERC 72-11 "Literature Survey - Seismic Effects on Highway Bridges," by T. Iwasaki, J. Penzien and R.W. Clough - 1972 (PB 215 613)A19
- EERC 72-12 "SHAKE-A Computer Program for Earthquake Response Analysis of Horizontally Layered Sites," by P.B. Schnabel and J. Lysmer - 1972 (PB 220 207)A06
- EERC 73-1 "Optimal Seismic Design of Multistory Frames," by V.V. Bertero and H. Kamil - 1973
- EERC 73-2 "Analysis of the Slides in the San Fernando Dams During the Earthquake of February 9, 1971," by H.B. Seed, K.L. Lee, I.M. Idriss and F. Makdissi - 1973 (PB 223 402)A14

- EERC 73-3 "Computer Aided Ultimate Load Design of Unbraced Multistory Steel Frames," by M.B. El-Hafez and G.H. Powell 1973 (PB 248 315)A09
- EERC 73-4 "Experimental Investigation into the Seismic Behavior of Critical Regions of Reinforced Concrete Components as Influenced by Moment and Shear," by M. Celebi and J. Penzien - 1973 (PB 215 884)A09
- EERC 73-5 "Hysteretic Behavior of Epoxy-Repaired Reinforced Concrete Beams," by M. Celebi and J. Penzien - 1973 (PB 239 568)A03
- EERC 73-6 "General Purpose Computer Program for Inelastic Dynamic Response of Plane Structures," by A. Kanaan and G.H. Powell - 1973 (PB 221 260)A08
- EERC 73-7 "A Computer Program for Earthquake Analysis of Gravity Dams Including Reservoir Interaction," by P. Chakrabarti and A.K. Chopra - 1973 (AD 766 271)A04
- EERC 73-8 "Behavior of Reinforced Concrete Deep Beam-Column Subassemblages Under Cyclic Loads," by O. Küstü and J.G. Bouwkamp - 1973 (PB 246 117)A12
- EERC 73-9 "Earthquake Analysis of Structure-Foundation Systems," by A.K. Vaish and A.K. Chopra - 1973 (AD 766 272)A07
- EERC 73-10 "Deconvolution of Seismic Response for Linear Systems," by R.B. Reimer - 1973 (PB 227 179)A08
- EERC 73-11 "SAP IV: A Structural Analysis Program for Static and Dynamic Response of Linear Systems," by K.-J. Bathe, E.L. Wilson and F.E. Peterson - 1973 (PB 221 967)A09
- EERC 73-12 "Analytical Investigations of the Seismic Response of Long, Multiple Span Highway Bridges," by W.S. Tseng and J. Penzien - 1973 (PB 227 816)A10
- EERC 73-13 "Earthquake Analysis of Multi-Story Buildings Including Foundation Interaction," by A.K. Chopra and J.A. Gutierrez - 1973 (PB 222 970)A03
- EERC 73-14 "ADAP: A Computer Program for Static and Dynamic Analysis of Arch Dams," by R.W. Clough, J.M. Raphael and S. Mojtahedi - 1973 (PB 223 763)A09
- EERC 73-15 "Cyclic Plastic Analysis of Structural Steel Joints," by R.B. Pinkney and R.W. Clough - 1973 (PB 226 843)A08
- EERC 73-16 "QHAD-4: A Computer Program for Evaluating the Seismic Response of Soil Structures by Variable Damping Finite Element Procedures," by I.M. Idriss, J. Lysmer, R. Hwang and H.B. Seed - 1973 (PB 229 424)A05
- EERC 73-17 "Dynamic Behavior of a Multi-Story Pyramid Shaped Building," by R.M. Stephen, J.P. Hollings and J.G. Bouwkamp - 1973 (PB 240 718)A06
- EERC 73-18 "Effect of Different Types of Reinforcing on Seismic Behavior of Short Concrete Columns," by V.V. Bertero, J. Hollings, O. Küstü, R.M. Stephen and J.G. Bouwkamp - 1973
- EERC 73-19 "Olive View Medical Center Materials Studies, Phase I," by B. Bresler and V.V. Bertero - 1973 (PB 235 986)A06
- EERC 73-20 "Linear and Nonlinear Seismic Analysis Computer Programs for Long Multiple-Span Highway Bridges," by W.S. Tseng and J. Penzien - 1973
- EERC 73-21 "Constitutive Models for Cyclic Plastic Deformation of Engineering Materials," by J.M. Kelly and P.P. Gillis 1973 (PB 226 024)A03
- EERC 73-22 "DRAIN - 2D User's Guide," by G.H. Powell - 1973 (PB 227 016)A05
- EERC 73-23 "Earthquake Engineering at Berkeley - 1973," (PB 226 033)A11
- EERC 73-24 Unassigned
- EERC 73-25 "Earthquake Response of Axisymmetric Tower Structures Surrounded by Water," by C.Y. Liaw and A.K. Chopra 1973 (AD 773 052)A09
- EERC 73-26 "Investigation of the Failures of the Olive View Stairtowers During the San Fernando Earthquake and Their Implications on Seismic Design," by V.V. Bertero and R.G. Collins - 1973 (PB 235 106)A13
- EERC 73-27 "Further Studies on Seismic Behavior of Steel Beam-Column Subassemblages," by V.V. Bertero, H. Krawinkler and E.P. Popov - 1973 (PB 234 172)A06
- EERC 74-1 "Seismic Risk Analysis," by C.S. Oliveira - 1974 (PB 235 920)A06
- EERC 74-2 "Settlement and Liquefaction of Sands Under Multi-Directional Shaking," by R. Pyke, C.K. Chan and H.B. Seed 1974
- EERC 74-3 "Optimum Design of Earthquake Resistant Shear Buildings," by D. Ray, K.S. Pister and A.K. Chopra - 1974 (PB 231 172)A06
- EERC 74-4 "LUSH - A Computer Program for Complex Response Analysis of Soil-Structure Systems," by J. Lysmer, T. Udaka, H.B. Seed and R. Hwang - 1974 (PB 236 796)A05

- EERC 74-5 "Sensitivity Analysis for Hysteretic Dynamic Systems: Applications to Earthquake Engineering," by D. Ray 1974 (PB 233 213)A06
- EERC 74-6 "Soil Structure Interaction Analyses for Evaluating Seismic Response," by H.B. Seed, J. Lysmer and R. Hwang 1974 (PB 236 519)A04
- EERC 74-7 Unassigned
- EERC 74-8 "Shaking Table Tests of a Steel Frame - A Progress Report," by R.W. Clough and D. Tang - 1974 (PB 240 869)A03
- EERC 74-9 "Hysteretic Behavior of Reinforced Concrete Flexural Members with Special Web Reinforcement," by V.V. Bertero, E.P. Popov and T.Y. Wang - 1974 (PB 236 797)A07
- EERC 74-10 "Applications of Reliability-Based, Global Cost Optimization to Design of Earthquake Resistant Structures," by E. Vitiello and K.S. Pister - 1974 (PB 237 231)A06
- EERC 74-11 "Liquefaction of Gravelly Soils Under Cyclic Loading Conditions," by R.T. Wong, H.B. Seed and C.K. Chan 1974 (PB 242 042)A03
- EERC 74-12 "Site-Dependent Spectra for Earthquake-Resistant Design," by H.B. Seed, C. Ugas and J. Lysmer - 1974 (PB 240 953)A03
- EERC 74-13 "Earthquake Simulator Study of a Reinforced Concrete Frame," by P. Hidalgo and R.W. Clough - 1974 (PB 241 944)A13
- EERC 74-14 "Nonlinear Earthquake Response of Concrete Gravity Dams," by N. Pal - 1974 (AD/A 006 583)A06
- EERC 74-15 "Modeling and Identification in Nonlinear Structural Dynamics - I. One Degree of Freedom Models," by N. Distefano and A. Rath - 1974 (PB 241 548)A06
- EERC 75-1 "Determination of Seismic Design Criteria for the Dumbarton Bridge Replacement Structure, Vol. I: Description, Theory and Analytical Modeling of Bridge and Parameters," by F. Baron and S.-H. Pang - 1975 (PB 259 407)A15
- EERC 75-2 "Determination of Seismic Design Criteria for the Dumbarton Bridge Replacement Structure, Vol. II: Numerical Studies and Establishment of Seismic Design Criteria," by F. Baron and S.-H. Pang - 1975 (PB 259 408)A11 (For set of EERC 75-1 and 75-2 (PB 259 406))
- EERC 75-3 "Seismic Risk Analysis for a Site and a Metropolitan Area," by C.S. Oliveira - 1975 (PB 248 134)A09
- EERC 75-4 "Analytical Investigations of Seismic Response of Short, Single or Multiple-Span Highway Bridges," by M.-C. Chen and J. Penzien - 1975 (PB 241 454)A09
- EERC 75-5 "An Evaluation of Some Methods for Predicting Seismic Behavior of Reinforced Concrete Buildings," by S.A. Mahin and V.V. Bertero - 1975 (PB 246 306)A16
- EERC 75-6 "Earthquake Simulator Study of a Steel Frame Structure, Vol. I: Experimental Results," by R.W. Clough and D.T. Tang - 1975 (PB 243 981)A13
- EERC 75-7 "Dynamic Properties of San Bernardino Intake Tower," by D. Rea, C.-Y. Liaw and A.K. Chopra - 1975 (AD/A008 406) A05
- EERC 75-8 "Seismic Studies of the Articulation for the Dumbarton Bridge Replacement Structure, Vol. I: Description, Theory and Analytical Modeling of Bridge Components," by F. Baron and R.E. Hamati - 1975 (PB 251 539)A07
- EERC 75-9 "Seismic Studies of the Articulation for the Dumbarton Bridge Replacement Structure, Vol. 2: Numerical Studies of Steel and Concrete Girder Alternates," by F. Baron and R.E. Hamati - 1975 (PB 251 540)A10
- EERC 75-10 "Static and Dynamic Analysis of Nonlinear Structures," by D.P. Mondkar and G.H. Powell - 1975 (PB 242 434)A08
- EERC 75-11 "Hysteretic Behavior of Steel Columns," by E.P. Popov, V.V. Bertero and S. Chandramouli - 1975 (PB 252 365)A11
- EERC 75-12 "Earthquake Engineering Research Center Library Printed Catalog," - 1975 (PB 243 711)A26
- EERC 75-13 "Three Dimensional Analysis of Building Systems (Extended Version)," by E.L. Wilson, J.P. Hollings and H.H. Dovey - 1975 (PB 243 989)A07
- EERC 75-14 "Determination of Soil Liquefaction Characteristics by Large-Scale Laboratory Tests," by P. De Alba, C.K. Chan and H.B. Seed - 1975 (NUREG 0027)A08
- EERC 75-15 "A Literature Survey - Compressive, Tensile, Bond and Shear Strength of Masonry," by R.L. Mayes and R.W. Clough - 1975 (PB 246 292)A10
- EERC 75-16 "Hysteretic Behavior of Ductile Moment Resisting Reinforced Concrete Frame Components," by V.V. Bertero and E.P. Popov - 1975 (PB 246 388)A05
- EERC 75-17 "Relationships Between Maximum Acceleration, Maximum Velocity, Distance from Source, Local Site Conditions for Moderately Strong Earthquakes," by H.B. Seed, R. Murarka, J. Lysmer and I.M. Idriss - 1975 (PB 248 172)A03
- EERC 75-18 "The Effects of Method of Sample Preparation on the Cyclic Stress-Strain Behavior of Sands," by J. Mulilis, C.K. Chan and H.B. Seed - 1975 (Summarized in EERC 75-28)

- EERC 75-19 "The Seismic Behavior of Critical Regions of Reinforced Concrete Components as Influenced by Moment, Shear and Axial Force," by M.B. Atalay and J. Penzien - 1975 (PB 258 842)A11
- EERC 75-20 "Dynamic Properties of an Eleven Story Masonry Building," by R.M. Stephen, J.P. Hollings, J.G. Bouwkamp and D. Jurukovski - 1975 (PB 246 945)A04
- EERC 75-21 "State-of-the-Art in Seismic Strength of Masonry - An Evaluation and Review," by R.L. Mayes and R.W. Clough 1975 (PB 249 040)A07
- EERC 75-22 "Frequency Dependent Stiffness Matrices for Viscoelastic Half-Plane Foundations," by A.K. Chopra, P. Chakrabarti and G. Dasgupta - 1975 (PB 248 121)A07
- EERC 75-23 "Hysteretic Behavior of Reinforced Concrete Framed Walls," by T.Y. Wong, V.V. Bertero and E.P. Popov - 1975
- EERC 75-24 "Testing Facility for Subassemblages of Frame-Wall Structural Systems," by V.V. Bertero, E.P. Popov and T. Endo - 1975
- EERC 75-25 "Influence of Seismic History on the Liquefaction Characteristics of Sands," by H.B. Seed, K. Mori and C.K. Chan - 1975 (Summarized in EERC 75-28)
- EERC 75-26 "The Generation and Dissipation of Pore Water Pressures during Soil Liquefaction," by H.B. Seed, P.P. Martin and J. Lysmer - 1975 (PB 252 648)A03
- EERC 75-27 "Identification of Research Needs for Improving Aseismic Design of Building Structures," by V.V. Bertero 1975 (PB 248 136)A05
- EERC 75-28 "Evaluation of Soil Liquefaction Potential during Earthquakes," by H.B. Seed, I. Arango and C.K. Chan - 1975 (NUREG 0026)A13
- EERC 75-29 "Representation of Irregular Stress Time Histories by Equivalent Uniform Stress Series in Liquefaction Analyses," by H.B. Seed, I.M. Idriss, F. Makdisi and N. Banerjee - 1975 (PB 252 635)A03
- EERC 75-30 "FLUSH - A Computer Program for Approximate 3-D Analysis of Soil-Structure Interaction Problems," by J. Lysmer, T. Udaka, C.-F. Tsai and H.B. Seed - 1975 (PB 259 332)A07
- EERC 75-31 "ALUSH - A Computer Program for Seismic Response Analysis of Axisymmetric Soil-Structure Systems," by E. Berger, J. Lysmer and H.B. Seed - 1975
- EERC 75-32 "TRIP and TRAVEL - Computer Programs for Soil-Structure Interaction Analysis with Horizontally Travelling Waves," by T. Udaka, J. Lysmer and H.B. Seed - 1975
- EERC 75-33 "Predicting the Performance of Structures in Regions of High Seismicity," by J. Penzien - 1975 (PB 248 130)A03
- EERC 75-34 "Efficient Finite Element Analysis of Seismic Structure - Soil - Direction," by J. Lysmer, H.B. Seed, T. Udaka, R.N. Hwang and C.-F. Tsai - 1975 (PB 253 570)A03
- EERC 75-35 "The Dynamic Behavior of a First Story Girder of a Three-Story Steel Frame Subjected to Earthquake Loading," by R.W. Clough and L.-Y. Li - 1975 (PB 248 841)A05
- EERC 75-36 "Earthquake Simulator Study of a Steel Frame Structure, Volume II - Analytical Results," by D.T. Tang - 1975 (PB 252 926)A10
- EERC 75-37 "ANSR-I General Purpose Computer Program for Analysis of Non-Linear Structural Response," by D.P. Mondkar and G.H. Powell - 1975 (PB 252 386)A08
- EERC 75-38 "Nonlinear Response Spectra for Probabilistic Seismic Design and Damage Assessment of Reinforced Concrete Structures," by M. Murakami and J. Penzien - 1975 (PB 259 530)A05
- EERC 75-39 "Study of a Method of Feasible Directions for Optimal Elastic Design of Frame Structures Subjected to Earthquake Loading," by N.D. Walker and K.S. Pister - 1975 (PB 257 781)A06
- EERC 75-40 "An Alternative Representation of the Elastic-Viscoelastic Analogy," by G. Dasgupta and J.L. Sackman - 1975 (PB 252 173)A03
- EERC 75-41 "Effect of Multi-Directional Shaking on Liquefaction of Sands," by H.B. Seed, R. Pyke and G.R. Martin - 1975 (PB 258 781)A03
- EERC 76-1 "Strength and Ductility Evaluation of Existing Low-Rise Reinforced Concrete Buildings - Screening Method," by T. Okada and B. Bresler - 1976 (PB 257 906)A11
- EERC 76-2 "Experimental and Analytical Studies on the Hysteretic Behavior of Reinforced Concrete Rectangular and T-Beams," by S.-Y.M. Ma, E.P. Popov and V.V. Bertero - 1976 (PB 260 843)A12
- EERC 76-3 "Dynamic Behavior of a Multistory Triangular-Shaped Building," by J. Petrovski, R.M. Stephen, E. Gartenbaum and J.G. Bouwkamp - 1976
- EERC 76-4 "Earthquake Induced Deformations of Earth Dams," by N. Serff and H.B. Seed - 1976

- EERC 76-5 "Analysis and Design of Tube-Type Tall Building Structures," by H. de Clercq and G.H. Powell - 1976 (PB 252 220) A10
- EERC 76-6 "Time and Frequency Domain Analysis of Three-Dimensional Ground Motions, San Fernando Earthquake," by T. Kubo and J. Penzien (PB 260 556)A11
- EERC 76-7 "Expected Performance of Uniform Building Code Design Masonry Structures," by R.L. Mayes, Y. Omote, S.W. Chen and R.W. Clough - 1976
- EERC 76-8 "Cyclic Shear Tests on Concrete Masonry Piers," Part I - Test Results," by R.L. Mayes, Y. Omote and R.W. Clough - 1976 (PB 264 424)A06
- EERC 76-9 "A Substructure Method for Earthquake Analysis of Structure - Soil Interaction," by J.A. Gutierrez and A.K. Chopra - 1976 (PB 257 783)A08
- EERC 76-10 "Stabilization of Potentially Liquefiable Sand Deposits using Gravel Drain Systems," by H.B. Seed and J.R. Booker - 1976 (PB 258 820)A04
- EERC 76-11 "Influence of Design and Analysis Assumptions on Computed Inelastic Response of Moderately Tall Frames," by G.H. Powell and D.G. Row - 1976
- EERC 76-12 "Sensitivity Analysis for Hysteretic Dynamic Systems: Theory and Applications," by D. Ray, K.S. Pister and E. Polak - 1976 (PB 262 859)A04
- EERC 76-13 "Coupled Lateral Torsional Response of Buildings to Ground Shaking," by C.L. Kan and A.K. Chopra - 1976 (PB 257 907)A09
- EERC 76-14 "Seismic Analyses of the Banco de America," by V.V. Bertero, S.A. Mahin and J.A. Hollings - 1976
- EERC 76-15 "Reinforced Concrete Frame 2: Seismic Testing and Analytical Correlation," by R.W. Clough and J. Gidwani - 1976 (PB 261 323)A08
- EERC 76-16 "Cyclic Shear Tests on Masonry Piers, Part II - Analysis of Test Results," by R.L. Mayes, Y. Omote and R.W. Clough - 1976
- EERC 76-17 "Structural Steel Bracing Systems: Behavior Under Cyclic Loading," by E.P. Popov, K. Takanashi and C.W. Roeder - 1976 (PB 260 715)A05
- EERC 76-18 "Experimental Model Studies on Seismic Response of High Curved Overcrossings," by D. Williams and W.G. Godden - 1976
- EERC 76-19 "Effects of Non-Uniform Seismic Disturbances on the Dumbarton Bridge Replacement Structure," by F. Baron and R.E. Hamati - 1976
- EERC 76-20 "Investigation of the Inelastic Characteristics of a Single Story Steel Structure Using System Identification and Shaking Table Experiments," by V.C. Matzen and H.D. McNiven - 1976 (PB 258 453)A07
- EERC 76-21 "Capacity of Columns with Splice Imperfections," by E.P. Popov, R.M. Stephen and R. Philbrick - 1976 (PB 260 378)A04
- EERC 76-22 "Response of the Olive View Hospital Main Building during the San Fernando Earthquake," by S. A. Mahin, R. Collins, A.K. Chopra and V.V. Bertero - 1976
- EERC 76-23 "A Study on the Major Factors Influencing the Strength of Masonry Prisms," by N.M. Mostaghel, R.L. Mayes, R. W. Clough and S.W. Chen - 1976
- EERC 76-24 "GADFLEA - A Computer Program for the Analysis of Pore Pressure Generation and Dissipation during Cyclic or Earthquake Loading," by J.R. Booker, M.S. Rahman and H.B. Seed - 1976 (PB 263 947)A04
- EERC 76-25 "Rehabilitation of an Existing Building: A Case Study," by B. Bresler and J. Axley - 1976
- EERC 76-26 "Correlative Investigations on Theoretical and Experimental Dynamic Behavior of a Model Bridge Structure," by K. Kawashima and J. Penzien - 1976 (PB 263 388)A11
- EERC 76-27 "Earthquake Response of Coupled Shear Wall Buildings," by T. Srichatrapimuk - 1976 (PB 265 157)A07
- EERC 76-28 "Tensile Capacity of Partial Penetration Welds," by E.P. Popov and R.M. Stephen - 1976 (PB 262 899)A03
- EERC 76-29 "Analysis and Design of Numerical Integration Methods in Structural Dynamics," by H.M. Hilber - 1976 (PB 264 410)A06
- EERC 76-30 "Contribution of a Floor System to the Dynamic Characteristics of Reinforced Concrete Buildings," by L.J. Edgar and V.V. Bertero - 1976
- EERC 76-31 "The Effects of Seismic Disturbances on the Golden Gate Bridge," by F. Baron, M. Arikan and R.E. Hamati - 1976
- EERC 76-32 "Infilled Frames in Earthquake Resistant Construction," by R.E. Klingner and V.V. Bertero - 1976 (PB 265 892)A13

- UCB/EERC-77/01 "PLUSH - A Computer Program for Probabilistic Finite Element Analysis of Seismic Soil-Structure Interaction," by M.P. Romo Organista, J. Lysmer and H.B. Seed - 1977
- UCB/EERC-77/02 "Soil-Structure Interaction Effects at the Humboldt Bay Power Plant in the Ferndale Earthquake of June 7, 1975," by J.E. Valera, H.B. Seed, C.F. Tsai and J. Lysmer - 1977 (PB 265 795)A04
- UCB/EERC-77/03 "Influence of Sample Disturbance on Sand Response to Cyclic Loading," by K. Mori, H.B. Seed and C.K. Chan - 1977 (PB 267 352)A04
- UCB/EERC-77/04 "Seismological Studies of Strong Motion Records," by J. Shoja-Taheri - 1977 (PB 269 655)A10
- UCB/EERC-77/05 "Testing Facility for Coupled-Shear Walls," by L. Li-Hyung, V.V. Bertero and E.P. Popov - 1977
- UCB/EERC-77/06 "Developing Methodologies for Evaluating the Earthquake Safety of Existing Buildings," by No. 1 - B. Bresler; No. 2 - B. Bresler, T. Okada and D. Zisling; No. 3 - T. Okada and B. Bresler; No. 4 - V.V. Bertero and B. Bresler - 1977 (PB 267 354)A08
- UCB/EERC-77/07 "A Literature Survey - Transverse Strength of Masonry Walls," by Y. Omote, R.L. Mayes, S.W. Chen and R.W. Clough - 1977
- UCB/EERC-77/08 "DRAIN-TABS: A Computer Program for Inelastic Earthquake Response of Three Dimensional Buildings," by R. Guendelman-Israel and G.H. Powell - 1977 (PB 270 693)A07
- UCB/EERC-77/09 "SUBWALL: A Special Purpose Finite Element Computer Program for Practical Elastic Analysis and Design of Structural Walls with Substructure Option," by D.Q. Le, H. Peterson and E.P. Popov - 1977 (PB 270 567)A05
- UCB/EERC-77/10 "Experimental Evaluation of Seismic Design Methods for Broad Cylindrical Tanks," by D.P. Clough
- UCB/EERC-77/11 "Earthquake Engineering Research at Berkeley - 1976," - 1977
- UCB/EERC-77/12 "Automated Design of Earthquake Resistant Multistory Steel Building Frames," by N.D. Walker, Jr. - 1977
- UCB/EERC-77/13 "Concrete Confined by Rectangular Hoops Subjected to Axial Loads," by D. Zallnas, V.V. Bertero and E.P. Popov - 1977
- UCB/EERC-77/14 "Seismic Strain Induced in the Ground During Earthquakes," by Y. Sugimura - 1977

